We would like to thank again both referees and Dr. Guyot for their valuable comments and suggestions. Bellow, are our responses to the comments together with changes in the revised manuscript. The marked-up version of the manuscript, attached at the end of this final response, does not include changes in the structure (order of subsections). The revisions in the structure are reported separately instead in Section 4 of this response.

1. Response to dr. Guyot

General comments

1) The introduction covers most important aspects but it omits to mention that attenuation by rainfall at these frequencies (E-Band) has already been investigated experimentally, e.g. by Shresta and Choi (2017) or Norouzian et al. (2020) for instance (and maybe other papers). This literature is often going under the radar of the atmospheric community maybe because it is published in specific engineering and electronics journals (often IEEE). Yes, the objective of these studies was the optimal design of back-haul networks, as to minimise the occurrence of signal fading, instead of opportunistic measurement of rainfall. But nethertheless, experimentally this is the same setup and collected data, and often even formulations and theoretical approaches. I would include a mention of their existence in the introduction, and eventually in the discussion if appropriate.

This is an interesting point. We are aware of E-band investigation being reported in the electrical engineering journals (often IEEE) and refer to two examples of this work in the Introduction (Hansryd et al., 2010; Luini et al., 2018) and two other examples in the section about wet antenna attenuation (section 2.4) (Hong et al., 2017; Ostrometzky et al., 2018). The investigations of Hansryd et al. (2010) and Luini et al. (2018) have similar scope as the papers suggested by Dr. Guyot. We have been considering also referring to other works, nevertheless, the propagation studies aiming at community designing microwave link networks are mostly focused on long-term availability and lack evaluation in shorter time scales, which is critical for evaluating retrieval of atmospheric variables. We thus believe, that our relatively concise list of references on radio engineering investigations suffices as it, first, covers most important topics being previously investigated and, secondly, can provide further reading through referenced or citing studies. On the other hand, we might have missed some important point in the suggested references or some topic in the radio engineering literature and will be thus happy for a notice.

2) L105: Which parameters values for the canting angle and temperature, and which model did you use for the T-Matrix calculations? You have to specify it here.

Thank you for notifying us of missing piece of information. We have provided this information in the revised manuscript in section 3.4:

"The extinction cross-sections used in Eq. (5) are calculated using Python implementation of T-matrix model (Leinonen, 2014). The calculation assumes temperature 10° C, canting angle 0°, drop shape being oblate spheroid, drop-axis ratio according to Pruppacher and Beard, (1970), and for drops smaller than 0.5 mm heuristic approximation of Pruppbacher and Beard formula is used."

3) Effect of the k-R relation on the retrievals. Those are interesting results but I think the paper abstract does not reflect the actual results of this section. Typically, in Table 5: the performance criteria are actually quite similar between the use of ITU parameters and DSD parameters. Often only 0.01 differs for R2, and RMSE rarely exceeds 0.05mm h-1. So only based on this, one might think the parameters used are not of real matter. But when looking at Table 4 and the parameters per rain type (stratiform and

convective, low and moderate rain rates) one sees the discrepancies. So it is the k-R relations for local DSD and differentiation for specific rain classes/types being used that has an impact on the retrievals at these frequencies. When lumped all together, ITU or specific DSD actually lead to similar retrievals outcomes. As the authors noted, including larger rain rates in the dataset would increase the differences in retrievals and the importance of the DSD on the retrievals at these rain rates.

The conclusions about sensitivity to drop size distribution are based on theoretical evaluation using attenuation and rainfall calculated from drop size distribution data. The effect of DSD is also demonstrated on real commercial microwave links (CMLs), nevertheless, other sources of errors, especially wet antenna attenuation (WAA) affect these results significantly. Moreover, our results are affected by the absence of heavy rainfalls during the experimental period (see Discussion section L589 – 595 of the original manuscript). This is the reason why only the longest CML is suitable for demonstrating DSD related errors. The shorter CMLs are overly affected by WAA during light rainfalls to enable interpretations on DSD errors. We might stress this also when referring to Table 5 or at another place in the manuscript to avoid confusion.
We are, however, convinced that results from the long CML are capable of demonstrating benefit of using parameters specifically derived for stratiform rainfalls. Although the improvement in the metrics is not large in absolute values it is significant in relative values. E.g. decrease in RMSE from 0.49 to 0.39 mm h^{-1} by 73.5 GHz sub-link and from 0.31 to 0.24 mm h^{-1} by 83.5 GHz sub-link is decreased by 20 % resp. 23 %. This is even more pronounced in relative error where improvement from -0.44 to -0.35 by 73.5 GHz sub-link and -0.17 to -0.08 by 83.5 GHz sub-link is an improvement by 20 % resp. 53 %.

Also based on comments of referee 2, we have revised Rainfall estimation subsection (now 4.4) and extended description of the results obtained from CMLs:

"The model with DSD-derived parameters improves performance with respect to all metrics. Sub-link 1147 1a also remains significantly underestimated with DSD-derived parameters. This is due to deficits in the baseline and WAA identification. The underestimation is pronounced especially during very light rainfalls with rainfall intensities under 1 mm h^{-1}, which represent 25% of total rainfall dept. Shorter CMLs are less sensitive to rainfall along their shorter path and are more affected by deficiencies in the estimated baseline and WAA. Thus, use of DSD parameters does not significantly improve performance of short CMLs. CMLs shorter than 1 km overestimate rainfall intensities more than longer CMLs. "

4) At these frequencies, longer CML path lengths translates in higher sensitivities to light rainfall – but it also means a coarser spatial resolution for CML rainfall maps – this can be a drawback and can be highlighted.

The higher sensitivity of longer CMLs to total rainfall attention is intrinsic to all frequency regions and the investigation of rainfall reconstruction goes beyond the scope of this study. Investigation addressing specifically CML rainfall reconstruction errors is presented for example in Rios Gaona et al. (2015).

Specific technical comments

We would like to thank Dr. Guyot for tracking our manuscript for typos and technical shortcomings as missing units or in several cases improper format of references. We have addressed all of them as suggested.

1) L52 Comma missing before "which"
Added.

2) L115 units of v(D)?
v(D) (m). Added.

3) L130 units of these variables?
Both are in cm^2.

4) L145 why not calling it the "Liebe model" as you did for the "Leijnse model"?
OK. Corrected.

5) Table 5: Instead of "Performance", use "performance metrics", or "evaluation criteria"?

6)There are a couple of instances in the paper when the citation format is not suitable, in particular l137 ". . .in (Liebe et al., 1993). . ." should be "in Liebe et al. (1993)". L166 has the same issue. L226 has the same issue. L263 has the same problem. L197 has the same issue.
Corrected.

7) "Parsivel" is an acronym and therefore should be written in Upper case letters, e.g. PARSIVEL
Corrected.

8) L238 Dm is in mm
Yes. Corrected.

9) Figure 4 (b) there is a typo for "convective". The legend has the same citation format issue (brackets should only be around the date).
Corrected.

10) L265 and 265, keep a consistent spacing between value and units (\%). I think there should be a space.
Corrected.

11) L277 units of Aw? (dB km-1)
No. A_w is in dB. Added.

12) L290 units of Awconst?
A_{wconst} is in dB. Added.

13) Figure 7, the word "dry spells" seems cut at the bottom. Abbreviation for the month of November should be "Nov." if following the correct abbreviation, otherwise writing it in full could be actually better.
OK.

14) L497 chronological order for citations should be preferred
We use alphabetical order.

15) L571 "attention" should be "attenuation"
Corrected.

16) L 609 "by lower frequencies" "by" should be removed.
"by" replaced by "at".

2. Response to anonymous referee 1

1) Fig.1: in the caption "scattering efficiency" is mentioned. Clearly this is not the same as extinction efficieny. Please clarify.

Thank you for spotting this inconsistency. The figure as well as equation 6 describe extinction efficiency (Q_{ext}).

We have corrected the Figure labels, description of the equation, and also one occurrence in the introduction section.

2) Fig.2: I suspect there is something wrong here. I do not see why the water vapor attenuation should have a drop at 60 GHz. Is this affecting results later on???

We have checked our results and there is nothing wrong with it. Results are fully consistent with Liebe et al. (1993) and could be cross-checked by independent computer codes available on GitHub, e.g. https://github.com/cchwala/pyMPM. The attenuation due to water vapor is in here (as well as later on) defined as the difference between wet-air and dry-air attenuation under the same moist air pressure and temperature. Thus, also effect of water vapor on attenuation due to oxygen is considered as described in ITU-R, (2019), and formerly by Liebe et al. (1993): First, moist air pressure is the sum of dry-air pressure and partial water pressure, thus dry-air pressure decreases during humid conditions (under the assumption of the same moist air pressure). This leads to a decrease in attenuation by molecules of oxygen. Second, partial water vapor pressure influences the width of the oxygen spectral lines (pressure broadening) as it affects the rate of collisions between the molecules (eq. 5 and 6a in ITU-R (2019)). These two effects lead to a decrease in attenuation due to oxygen when water vapor content increases. This decrease can reach about 4 % for conditions with moist air pressure 1015 hPa, temperature 30° C, and 100 % air humidity. Such decrease has relatively negligible effect for frequencies used in this study (73-74 and 83-84 GHz). Nevertheless, it is not negligible around 60 GHz (as can be seen on Figure 2), where the attenuation due to oxygen dominates over attenuation directly caused by water vapor molecules.

We have clarified the definition of attenuation due to water vapor in the paragraph describing the Figure. We have also added an explanation how water vapor influences attenuation due to oxygen (L97 – 101 in the revised manuscript). Finally, the reference to ITU-R recommendations (ITU-R, 2016) has been updated to ITU-R (2019):

3) I find the narrative from 3.3 onwards (including Sect4) very difficult to follow. I would recommend to reshu so that for instance when you talk about Sensitivity of the k-R model to drop size distribution you cover the whole thing (including line 400-425). Same for the other bits (e.g. Quality check, Dry-wet weather classification, Baseline identification, Wet antenna attenuation). At the moment the reader need to jump back and forward because the logical thread is erratic. Also some topic (e.g. gas attenuation should come before rainfall retrieval because of course the effect of gas must be subtracted first!).

We thank for the suggestions on modifying the structure of the manuscript. First part of the comment suggests presenting jointly methods and results belonging to the one subtopic. However, we prefer to avoid the inclusion of results in the Materials and Methods section. Moreover, the research performed is multifocal, the use of subheadings within the Materials and Methods section, that are mirror-imaged in the Results section, is intended to make it easier for readers of the manuscript to associate which Materials and Methods are used to obtain which results. Furthermore, all the subtopics *(e.g. Quality check, Baseline*

identification, Wet antenna attenuation)' are part of the same processing chain and influence each other and thus it is in our view reasonable to present them together.

Regarding the second suggestion (re-order rainfall retrieval and gas attenuation), we agree that effect of gaseous attenuation influences baseline identification and can be presented earlier.

In the revised manuscript, we, firstly, present subsections related to gaseous attenuation before subsections related to effect of drop size distribution on attenuation-rainfall model and subsection related to rainfall estimation procedure. The order of subsections has been, therefore, changed in Sections 2, 3, 4, and 5 to maintain mirror-imaging of the topics within the sections. Secondly, separate subsection 3.6 Performance evaluation was removed and its content is presented within the other subsections of Method section. E.g. Performance evaluation related to gaseous attenuation is presented in the subsection about gaseous attenuation, etc. Thirdly, subsections referring to dry-wet weather classification and hardware related artifacts were moved to the appendices. Both of the topics are not critical to the conclusions but are in our view useful for experts utilizing CML data for rainfall retrieval. Finally, to further improve flow of the presentation, IDs of CMLs were simplified to numbers from 1 to 6 with suffices "a" and "b" (e.g. 1a and 1b) when referring to 73-74 GHz resp. 83-84 GHz sub-links.

4) Eq.10 and Fig.4b. Where is this coming from? I have never seen such a relationship between an intensive quantity like RR and D_M!!!!!

The parameters of theoretical functions describing drop size distribution (DSD) are scaled to rainfall intensity, as can be seen in Figure 4a. In this particular case, gamma distribution as proposed by Ulbrich (1983) is used. Thus, mass-weighted diameters (ratio between 4^{th} and 3^{rd} DSD moments) need to be also scaled to rainfall intensity, as shown in Figure 4b. The scaling procedure is explained in the paragraph above the eq. 10 (lines 224-226 of the original manuscript) and adequately referenced to the benchmark paper of Ulbrich (1983).

5) Table 3: you are introducing parameters (epsilon, delta,) that are not defined anywhere.

The parameters are taken from Table 2 in Ulbrich (1983). The paper was cited in the Table caption of the original manuscript. We have added details on each parameter to the Table:

"N_0 ($m^{-3}cm^{-1-\mu}$) and μ (-) are parameters of semi-empirical gamma distribution function, ε ($h^{-\delta}$) and δ (-) are scaling parameters of this function."

6) I do not understand the rationale of doing the investigation with the "theoretical DSD" (not clear where they come from). On the other hand I see the point of using disdrometer data but I would recommend to use extensive datasets like available at https://ghrc.nsstc.nasa.gov/home/field-campaigns (and plot density functions instead of plotting scatterplots as in Fig.10). This should also allow to assess uncertainty errors due to DSD variability like done in Tab.4 in a more robust way.

Theoretical DSD enables us to show, that results based on observed DSD are consistent with results using widely acknowledged theoretical DSD functions, which in our opinion supports the conclusions and shows that the results are not only site-specific. When describing theoretical DSD, we use gamma distribution function scaled to rainfall intensity as suggested by Ulbrich (1983).

In our opinion, one year of DSD data from the well-controlled experiment is sufficient to demonstrate the effect of DSD on attenuation-rainfall power-law relation. The dataset was previously used in several papers in high-quality journals (e.g., Schleiss et al., 2013; Wang et al., 2012) and we had the dataset handy. Moreover, the dataset is from temperate climate and thus applicable also for our case study.

7) The authors mention stratiform vs convective precipitation coefficients. How do they practically envisage to separate stratiform vs convective precipitation?

The separation to convective and stratiform rainfalls is performed only in the investigation with theoretical and observed DSD (sections 3.3 and 4.4 of the original manuscript) to demonstrate that attenuation-rainfall relation is sensitive to rainfall type. The classification procedure is described in the section 3.3 of the original manuscript.

The separation of convective and stratiform rainfalls in practical applications is discussed in Discussion section of the original manuscript (L545-548). This section refers to the work of Leth et al. (2019). Unfortunately, detailed elaboration on possible methods for separation of convective and stratiform rainfalls is out of the scope of this manuscript.

8) Assuming that "rainfall has a uniform distribution over the study area, and that water formation on the surface of antenna radomes is the same for both the short CMLs and the long one" is quite an assumption! This approach is very provisional.

We agree that assumptions seem to be strong. Nevertheless, we believe that its appropriateness is, in our case, justified and was carefully discussed in Discussion section of the original manuscript (L511-518). Line of reasoning is briefly repeated below.

The rainfall spatial variability (in the studied period) is low: The correlation coefficient between 15-min rainfall observations of nearby rain gauges (rg_1 and rg_2) is 0.94–0.96. The correlation between these rain gauges and the more distant rain gauge rg_3 is still over 0.88.

Wet antenna attenuation (WAA): All the CML units are of the same type and have similar ages (deployed during 2016 and 2017). Furthermore, as discussed on L516-518 of the original manuscript, the procedure is in our case relatively insensitive to differences in antenna properties, because WAA is quantified by comparing short (0.4 – 1.4 km) CMLs by which WAA dominates over path attenuation, to the 4.86 km long CML, which is relatively insensitive to WAA even during light rainfalls. Satisfactory performance of the approach is also demonstrated in the Results section in Figure 7.

To further strengthen the arguments about the legitimacy of those assumptions, we have added an information on the age of the units into section 3.1 Experimental sites and instrumentation. Furthermore, Figure demonstrating the concept of WAA estimation on time series (Fig. 9a in the revised manuscript) was extended by a scatter plot (Fig. 9b) with regression lines relating observed attenuation during light and moderate rainfall to the length of sub-links.

9) "E-band CMLs are by about one order of magnitude more attenuated by raindrops along their path than older 15–40 GHz devices": this is a very vague (imprecise) statement also given the fact that attenuation at 40 GHz is already 6 times attenuation at 15 GHz!!!! Same for the sentence "Gaseous attenuation at E-band CMLs is detectable, however, it is two orders of magnitude smaller than attenuation due to rainfall" (again quite vague and approximate!)

Agreed. We will be more precise in our statements. We have modified the conclusions as follows:

- "E-band CMLs are markedly more attenuated by raindrops along their path than older 15–40 GHz devices, during lighter rainfalls by about 20 times more than 15 GHz and 2 - 3 times more than 40 GHz devices."

- "Gaseous attenuation at E-band CMLs is detectable, however, it is substantially smaller than attenuation due to rainfall. Fluctuations in specific attenuation caused by water vapor typically not exceed 1 dB km^{-1} in the region of temperate climate. This magnitude is reached by rainfall with intensity around 1 mm h^{-1}."

References:
ITU-R: ITU-R P.676-11, [online] Available from: https://www.itu.int/dms_pubrec/itu-r/rec/p/R-REC-P.676-11-201609-I!!PDF-E.pdf, 2016.

ITU-R: RECOMMENDATION ITU-R P.676-12 - Attenuation by atmospheric gases and related effects, [online] Available from: https://www.itu.int/dms_pubrec/itu-r/rec/p/R-REC-P.676-12-201908-I!!PDF-E.pdf, 2019.

Leth, T. C. van, Leijnse, H., Overeem, A. and Uijlenhoet, R.: Estimating raindrop size distributions using microwave link measurements, Atmospheric Measurement Techniques Discussions, 1–27, doi:https://doi.org/10.5194/amt-2019-51, 2019.

Liebe, H. J., Hufford, G. A. and Cotton, M. G.: Propagation modeling of moist air and suspended water/ice particles at frequencies below 1000 GHz. [online] Available from: http://adsabs.harvard.edu/abs/1993apet.agar.....L (Accessed 17 October 2019), 1993.

Schleiss, M., Rieckermann, J. and Berne, A.: Quantification and Modeling of Wet-Antenna Attenuation for Commercial Microwave Links, IEEE Geoscience and Remote Sensing Letters, 10(5), 1195–1199, doi:10.1109/LGRS.2012.2236074, 2013.

Ulbrich, C. W.: Natural Variations in the Analytical Form of the Raindrop Size Distribution, J. Climate Appl. Meteor., 22(10), 1764–1775, doi:10.1175/1520-0450(1983)022<1764:NVITAF>2.0.CO;2, 1983.

Wang, Z., Schleiss, M., Jaffrain, J., Berne, A. and Rieckermann, J.: Using Markov switching models to infer dry and rainy periods from telecommunication microwave link signals, Atmospheric Measurement Techniques, 5(7), 1847–1859, doi:10.5194/amt-5-1847-2012, 2012.

3. Response to the referee comment by Giacomo Roversi

The paper by Fencl et al. addresses a topical and interesting matter, as extends known opportunistic precipitation sensing techniques to the more recent E band links. It high-lights the new possibilities uncovered by the different frequencies and hardware and focuses on the consequent challenges. The authors give a complete picture of the subject from theory to application, preparing the ground for future studies. The article is therefore certainly valuable and of primary interest to the CML scientific community and AMT readers.

The work is well written and the goals defined in the abstract and introduction are all met. The discussion of the main issues is complete and rich, while some redundancy and repetitiveness is found in introductory and methodological sections, combined in certain cases with lack of the detailed quantitative information needed to contextualize some statements. Accordingly, a minor revision is suggested in order to provide the reader with more concise and relevant information in the cases treated in the comments below.

The author's answers to previous comments (AC1 and AC2 to SC1 and RC1 resp.) have been taken into consideration.

We have followed specific suggestions of the reviewer to remove identified redundancies and repetitiveness and provided additional quantitative information where required.

General comments

1) The fragmentation of the presentation as reported in comment 3. of RC1 is recognized: most of the topics are introduced in Sections 2 and 3 and then corroborated with quantitative data only in section 4 or even 5. Given the different data sets and methods utilized for the various steps of the investigation, the reading results some-times erratic indeed. However, the intentions declared by the authors (AC2) are also well understood. I will then strongly encourage a more widespread use of subsection cross referencing, to help the reader understand without changing the logical structure of the paper. An example of convenient referencing is found e.g. in L362 and 363. This should be replicated diffusely to connect introductory and discussion Sections. It seems to me that multipath disturbance instead is not introduced at all before L577 and should be added to Section 2 with some estimate of its magnitude.

Thank you for understanding to our intention to avoid inclusion of Results into Method and Material section. However, to make our presentation clearer we carefully identified redundancies and use more widespread cross-referencing as suggested. Furthermore, we have changed order of subsections and moved subsections related to dry-wet weather classification and hardware related artifacts into Appendices. More details are provided in our response to the comment no. 3 of anonymous referee 1.

In the revised version of the manuscript, we also introduced multipath disturbance (already in the Section 2.1, where different components of total observed loss are introduced).

2) Another downside of the chosen presentation layout is the need of re-introducing some aspects generally many times throughout the paper, without going quickly into the necessary detail. A more concise and unitary approach to the problems encountered and the solutions adopted would facilitate a global understanding of the work. I suggest therefore to support the introductory informations, in the first sections already, with quantitative informations and stating author's intentions regarding approximations and further discussions. In that way the reader could expect what to find in the next sections and repetitive recalls to the qualitative introduction would not be needed. Some non-exhaustive examples are reported below and most of the specific comments deal with this same issue. L74 to 78 - though the paragraph's introductory intent is clear, it lacks the detail and clearness about which assumptions are kept and which are discussed, with respect to previous 15-40 GHz approaches. L94 to 101 - It is not clear at this point how the authors will deal with the reported considerations further in the paper.

Our intention is to avoid inclusion of our original findings in section 1 and section 2. Section 1 provide general introduction with state-of-the art in microwave link rainfall estimation based upon which the goals of this manuscript are defined. Section 2 provides theoretical background enabling reader to follow our original methodology and results.

We would like to keep our original methodology and findings clearly separated and thus we want to avoid summary of our original findings already in the introductory sections. Similarly, we would like to keep our original methodology separated from theoretical background provided by previous works (section 2). Thus, although concept of baseline separation is introduced already in the Section 2 we prefer to explain how we approach this challenge in Section 3 - Material and Methods. Following the same intention, we prefer not to explain assumptions behind quantifying wet antenna attenuation in this work already at L94 – 101 of the original manuscript, but again in the Section 3.

To clarify this intention, we have modified the paragraph describing structure of the manuscript, specifically description of section 2 and 3: "Section 2 of the manuscript summarizes based upon previous

works the principles behind retrieving atmospheric variables from CML observations, Section 3 describes the methodology and datasets used in this manuscript for the assessment of E-band CMLs, …".

3) An additional figure showing WAA against link length could be used to illustrate the linear regressions proposed in Eq. 11 and the constant behaviour in dew cases. A sample of how the figure could look is attached.:

Agreed. We have shown such figure (Fig. 9b in the revised manuscript). Details are provided in the specific comments no. 11 and 17.

Specific comments (in order of appearance):

1) *L68 - Free space loss (Lbf) is said to be uniquely defined by distance and wavelength. Reporting the formula could be appropriate and helpful for further understanding of the discussion, as the frequency is a key variable for this study (E band).*

   Yes. We now report the formula of free space loss in the revised manuscript on line L68-70:

   "Free space loss L_{bf} is uniquely defined by the distance d (m) between the transmitter and receiver, and by wavelength λ (m):

   $L_{bf} = 20\left(\frac{4\pi d}{\lambda}\right)$"

2) *L74-78 - The phrase "Attenuation during dry weather is assumed to be a baseline" is apparently in direct contrast with the following "Fluctuations in the baseline during dry weather can be attributed..." if the reader does not know already the different magnitudes involved. Early introduction of orders of magnitude and average behaviours is therefore encouraged.*
   Agreed. We report typical magnitudes of rainfall and gaseous attenuation in the section 2.1, after description of different components of total observed loss (L72-75 in the revised manuscript).

3) *L101 - "More extensive investigations..." I think this sentence will state the motivation of the author's work, but it could be also interpreted as what still remains unknown after the work's results instead. Please clarify to avoid this ambivalence.*

   The sentence indeed stated our motivation. The motivation was, however, presented already at the end of Section 1. We have, therefore, deleted this sentence to avoid misunderstanding. Furthermore, we express at the end of the Introduction section, where structure of the manuscript is described, that section 2 provides review of previous work (see response 2 in the general comments).

4) *L131 - Fig. 4 is useful to the contextualisation of this sentence and should be referenced. "Contribute relatively less" is not gaugeable, some more detail may be added.*

   Agreed. We have referenced subsection 3.4, which contains Figure 4 (we would like to avoid referencing Figure 4 before Figure 3 is referenced). Nonetheless, we kindly disagree with the second suggestion. We would like to avoid detailed quantitative description in here. Reader can easily read quantitative information from the figure referenced in this sentence (Fig. 2 in the revised manuscript).

5) *L145 and following - The study on the components of N is not justified by following discussion or results and could be omitted as it lacks quantitative information. I think that the qualitative concept of the dependency of k to the various components is already* well *stressed.*

Agreed. As suggested, study on the components of N (lines 145-150 of the original manuscript) has been omitted in the revised version of the manuscript. Interested reader can find these details in the cited literature.

6) *L194 - "The periods for evaluating rainfall retrieval and for evaluating the effect of humidity and temperature fluctuations on gaseous attenuation are, therefore, different." The phrase itself is a quite obvious consequence of the previous sentence, while its implications are not. It should either be omitted or some expected implications should also be discussed (or at least some reference to the respective discussion should be made) in terms e.g. of which investigations are precluded by using different time windows.*

Agreed. The phrase is obvious and it has been deleted.

7) *L200 and other appearances of "aggregate" - it should be pointed out how the aggregation to different time scales is performed (mean, median, sum, max, other...)*

We aggregate to different time scales using mean. We have added this information into revised manuscript.

8) *L246 and 247 - The sentence is not clear and should be rephrased and expanded. "dependent" should perhaps be substituted with "depending", commas before and after "therefore" are not necessary and slow the reading. The threshold for Dm is not indicated.*

Thank you, for spotting this typo. This typo apparently led to misunderstanding. D_m as estimated by Eq. (11, in the revised manuscript) is actually the threshold which is used for classifying rainfalls. This threshold (D_m) is dependent on rainfall intensity.
We have changed the sentence to: "The approximation (Eq. 11) is used to calculate threshold for classifying disdrometer records as convective or stratiform. The threshold is dependent on rainfall intensity. Parameters *c* and *d* are estimated by fitting Eq. (11) to D_m as derived from real disdrometer data using Eq. (10)".

9) *L259 - Visual inspection does not seem like a robust approach to filter the outliers. Some technique should be at least suggested to cope with this kind of artefacts, as the visual approach is clearly not feasible at larger and near real-time scales.*

Visual check is indeed not a robust approach which could be used in future applications. The automation of quality check is, however, out the scope of this manuscript. Visual identification of artifacts is, in our view, first step towards future automation of this process. Moreover, the correction for artifacts is performed only in a single case. This correction is transparently reported (L260 of the original manuscript), to ensure reproducibility of the results.

10) *L269 - One-week sized moving window "is sufficiently short": are baseline drifts proven to happen only at longer time scales? Is the same for gaseous attenuation? Could it be that some higher frequency signal is masked by this approach resulting in the weakening of the water vapour detection capabilities?*

No, as reported on L260-261, also sudden change in baseline occur in the case of CML 3004_3005 (ID 2 in the revised manuscript) and this change was manually corrected. The baseline identification using one-week sized moving window is used only for rainfall retrieval. As reported on L305-306 of the original manuscript, constant baseline is used when analyzing effect of gaseous attenuation and potential for water vapor retrieval. Hardware related artifacts causing slow baseline drift have probably potential to destroy gaseous attenuation signal as discussed in the Discussion section (L581-584 in the original manuscript).

11) *L283 - A reference to Fig. 8 or to the suggested new figure could be added here.*

We have modified the figure in the revised manuscript according to reviewer's suggestion, however, we have at the end decided not to reference the figure at this place to keep the methods strictly separated from the results.

12) *L296 and 340 - Since Prague is located at an altitude around 200m (990 hPa), to as-sume the atmospheric pressure of 1013.25 hPa seems either systematically wrong or reported with too high precision (if differences between 990 and 1013 are negligible for the author purposes, then decimals of hPa are even more so). It is therefore suggested to utilize 990 hPa as reference pressure or at least replace the number with a more generic "at sea-level pressure".*

Agreed. We have replaced the number with more generic "sea-level pressure".

13) *L323 - Short CMLs are highlighted in some following sections as valuable tools for intense rainfall detection. Here instead the sentence "The performance ..." says that they will be presented only as examples of bad performance. Please clarify.*

Potential of short CMLs is highlighted in the Discussion section (L556 -562 of the original manuscript) in the context of observing heavy rainfalls associated with high spatial variability by which an assumption about uniform rainfall distribution along a CML path is more likely valid for short CMLs than for long ones. Nevertheless, only light and moderate rainfalls occurred during observation period. Short CMLs are, during these rainfalls relatively more affected by wet antenna attenuation than longer CMLs, as demonstrated e.g. on figure 7 in the original manuscript. The sentence, in the original manuscript actually states that: 'The performance of the short CMLs is shown to demonstrate limitations related to the improper baseline and WAA identification which are more pronounced by shorter CMLs.' This is in our view, not in contradiction with Discussion section, where shorter CMLs are suggested as valuable tool for detecting heavy rainfalls.

To avoid misunderstanding, we have modified the sentence to: 'The performance of the short CMLs is shown to demonstrate limitations related to the improper baseline and WAA identification which are, especially during light rainfalls, more pronounced by shorter CMLs.'

14) L347 to 358 - Is there any indication of what could cause the "degraded resolution" on the hardware side? If yes, it would be an interesting topic to read here.

In our opinion, the degraded resolution might be related to automatic power control. Nevertheless, this was not tested. We thus prefer to not speculate in this direction.

15) L365 and Fig. 6 - It should be reminded to the reader that sub-links belonging to one CML are presented in pairs in consecutive order. It should be consequently pointed out that intra-CML correlation creates 2x2 darker squares along the diagonal in the correlation matrix plot.

We have decided to change IDs of CMLs in the whole manuscript to better indicate sub-links belonging to the same CML and in general improve clarity of the whole manuscript: each CML have unique ID (numbers from 1 to 6). IDs of sub-links operating at 73 – 74 GHz and 83 – 84 GHz frequency then consist of CML ID and suffix "a" resp. "b".

Regarding intra-CML correlation, we believe, that the first sentence referring to the Figure 6 (Figure A1 in the revised manuscript) now provides sufficient guidance in this respect: "Dry-wet weather classifiers of single sub-links belonging to one CML are strongly correlated (Fig. A1)."

16) L369 - It is stated that the delay of the rain gauges in detecting rainfall with respect to CMLs "can be attributed to the delay of rain gauge rain detection due to the filling of the bucket." Please discuss whether delays and volume losses are compatible to the bucket size.

Thank you for this comment. We have removed this statement as it was based on analysis not shown in the manuscript and might have been considered speculative. The section will thus contain only results shown on figure A1 of the revised manuscript.

17) L377 to 380 - Same as L283, the dependency (and independence) of WAA to path length should be presented for rain (and no-rain) occurrences with a specific scatterplot and a linear fit (suggested figure attached).

Agreed. Figure 7 (9 in the revised manuscript) has been extended by a scatter plot showing relation between path length and total attenuation together with linear fits indicating effect of WAA.

18) Fig.7 - When comparing signals from CMLs of different path length, specific attenuation (dB/km) should be preferred to pure attenuation (dB). If the aim is to show the different regimes (dependency and independence to path length), then two plots should be shown (dB and dB/km time series), in order to appreciate inter-CML concordance on specific attenuation during rainfall and on pure attenuation during dry periods.

The signal shown in the figure 7 (Figure 9 in the revised manuscript) is predominantly caused by wet antenna attenuation, which is independent of path length. We therefore prefer to show exclusively total attenuation in this figure.

19) L405 - "However, it is closer ..." the reported considerations is interesting for an operational use and therefore valuable, but it is poorly proven (only visually). Without a gauge of the goodness of the

approximation (or some reference to following consistent results), the ITU fit may as well not be good for either case (convective and stratiform).

The attenuation-rainfall relation is for theoretical drop size distribution almost perfectly approximated by power-law fits (as reported on L400-401 of the original manuscript). Thus, distances between presented power-law curves (absolute errors) provide meaningful gauge of goodness. The term “it is closer” on L405 in the original manuscript describe distances between the curves. Thus, it is, in our opinion, appropriate. Moreover, reader can easily get information on approximate distances for any rainfall intensity between 0-50 mm/h from the figure 9 in the original manuscript. In addition, parameters of power-law fits as well as parameters obtained from ITU (ITU-R, 2005) are provided as a part of figure 9. Interested reader can thus easily express exact value of absolute errors for any rainfall intensity, resp. specific attenuation.

20) *L433 - To my understanding, it is the first time here that some speciific deficits in baseline and WAA identification for sub-link 1147 are asserted. It seems quite in contradiction with other parts of the text were the long CML has the best results.*

The sub-link 1147 (1b in the revised manuscript) clearly outperform shorter CMLs in terms of correlation (r = 0.96 and 0.97 compared to 0.53 – 0.86 resp. 0.61 – 0.87) and in terms of RMSE (0.39 and 0.24 mm h^{-1}compared to 0.64 – 2.18 resp. 0.69 – 1.44 mm h^{-1}), which can be seen in Table 5. Its markedly better performance is also clearly visible from the scatter plots in figure 11. The long CML cannot, however, accurately capture very light rainfalls under 1 mm h^{-1}, which represent about 25 % of the total rainfall depth in our case. We have added an information about underestimation of very light rainfalls to the revised manuscript at the place describing performance of the long CML (L434 - L435).

21) *L448, 449 and Fig. 12 - The anti-correlation of the attenuation with temperature is evident from figure 12b and should be highlighted here, as temperature seems to be the dominant component of the signal. Moreover, this appears in direct contradiction with what stated in the first paragraph of Section 4.6, so that may be reformulated differently.*

The negative correlation between attenuation and temperature appears in the figure, because water vapor density is strongly correlated with temperature. As gaseous attenuation is highly correlated to water vapor density, there is also strong (negative) correlation link between gaseous attenuation and temperature. It is, however, not caused by direct dependence, which is almost negligible: See ITU-R, (2019) and Figure 2 of the original manuscript.

22) *L515 - "The similarity in antenna characteristics was not inspected directly." Are the antenna factory features known to the authors? Is this sentence referring to technical specifications of the antennas or to the actual status of the radomes?*

The sentence refers to hydrophobic properties of antenna radomes as well as actual status of the radomes. It has been specified in the revised manuscript.

23) *Supplementary material - The ATPC (5th paragraph) is said to be "switched off" but, to mine understanding of Fig. S1, the concept of "saturated" may be more adherent to the case. It seems to me*

that ATPC can deal only with maximum 7 dB gains on tx, but it keeps working even there, in the sense that the gain remains 7 dB, while "ATPC switched off" is more likely a zero-gain scenario.

Yes, the ATPC keeps working in the sense it maintains *tx* power on the maximal (allowed) level. In the revised version of the supplementary material, we use the term 'saturated' instead 'switched off'.

Technical observations:

Figure 2 - It is not clear what the coloured bands represent (standard deviation or total spread) and neither is the direction from low to high pressure.

The color bands represent total spread. It is now clarified in the figure caption.

L202 and Table 2 - "Height" is used, but maybe "depth" is a more common choice to indicate precipitation amount.

Agreed. We now use the term 'depth'.

Fig. 6 - Raingauge labels differ between image and caption ("wet_" prefix)

Thank you for spotting this inconsistency. We have corrected it.

Fig. 8 - Since the two plot rows represent different frequency ranges, some labels indicating the two ranges are fostered to be shown to the left of the plot. Otherwise this information should at least appear in the caption with "upper row" and "lower row" indications.

We have added to the left two labels indicating frequency ranges.

L413 - I suggest the replacement of "heteroscedastic" with a more generic formulation, e.g. "the spread clearly grows with R and k". Although the adjective is certainly correct for a distribution like the one shown in Fig. 10, its use seems not proper for this context: given its precise statistical meaning and implications, I think it is preferable to run some specific tests of heteroscedasticity before asserting this property.

Done.

Fig. 12 - The colours for theoretical and observed attenuations are poorly chosen as they appear very similar (especially light green against light blue), both on paper and on screen.

OK, we have adjusted the colors to differentiate better the time series.

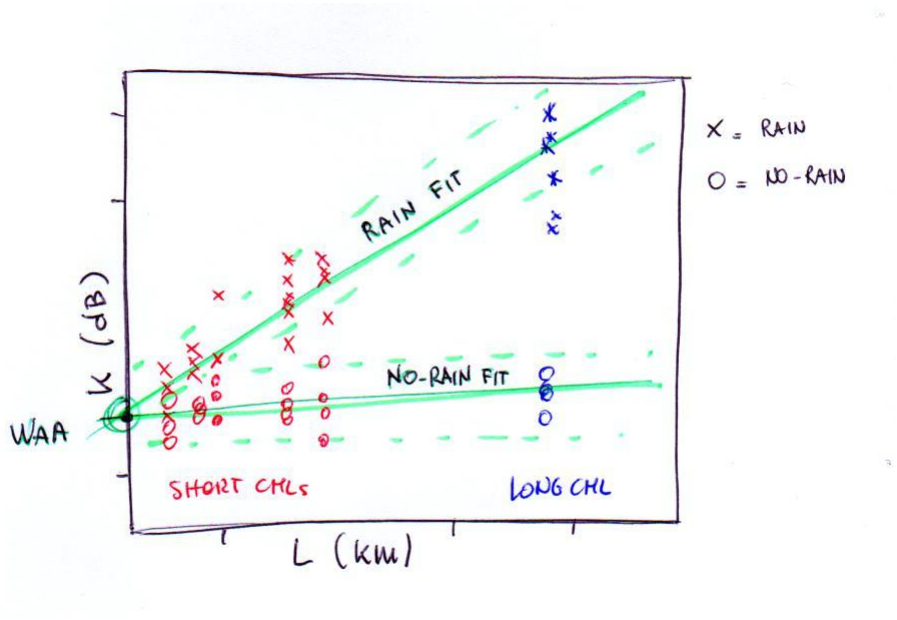

Fig. 1. Scatterplot of attenuation against pathlength with separated linear fits for rain and no-rain intervals (reviewer's suggestion).

References:

ITU-R: ITU-R P.838-3, [online] Available from: http://www.itu.int/dms_pubrec/itu-r/rec/p/R-REC-P.838-3-200503-I!!PDF-E.pdf, 2005.

ITU-R: RECOMMENDATION ITU-R P.676-12 - Attenuation by atmospheric gases and related effects, [online] Available from: https://www.itu.int/dms_pubrec/itu-r/rec/p/R-REC-P.676-12-201908-I!!PDF-E.pdf, 2019.

4. Revised structure of the manuscript

Revised structure of the manuscript as described in the comment no. 3 of the response to anonymous referee 1.

1 Introduction

2. Retrieving atmospheric variables from CMLs

2.1 Components of total observed loss

2.2 Attenuation by atmospheric gasses ~~Wet antenna attenuation~~

2.3 Relation between raindrop path attenuation and rainfall intensity

2.4 Wet antenna attenuation~~Attenuation by atmospheric gasses~~

3. Material and Methods

5. Marked-up version of the revised manuscript

Note, that the changes in the manuscript structure indicated above are not marked in the marked-up version of the revised manuscript presented on following pages.

Atmospheric observations with E-band microwave links – challenges and opportunities

Martin Fencl[1], Michal Dohnal[1], Pavel Valtr[2], Martin Grabner[3], Vojtěch Bareš[1]

[1]Department of Hydraulics and Hydrology, Czech Technical University in Prague, Prague 6, 166 29, Czech Republic
[2]Department of Electromagnetic Field, Czech Technical University in Prague, Prague 6, 166 29, Czech Republic
[3]Department of Frequency Engineering, Czech Metrology Institute, Brno, 638 00, Czech Republic

Correspondence to: Martin Fencl (martin.fencl@cvut.cz)

Abstract. Opportunistic sensing of rainfall and water vapor using commercial microwave links operated within cellular networks was conceived more than a decade ago. It has since been further investigated in numerous studies predominantly concentrating on the frequency region of 15–40 GHz. This manuscript provides the first evaluation of rainfall and water vapor sensing with microwave links operating at an E-band (specifically, 71–76 GHz and 81–86 GHz), which are increasingly updating, and frequently replacing, older communication infrastructure. Attenuation-rainfall relations are investigated theoretically on drop size distribution data. Furthermore, quantitative rainfall estimates from six microwave links, operated within cellular backhaul, are compared with observed rainfall intensities. Finally, the capability to detect water vapor is demonstrated on the longest microwave link measuring 4.86 km in path length. The results show that E-band microwave links are ~~by one order of magnitude~~markedly more sensitive to rainfall than devices operating in the 15–40 GHz range and are thus able to observe even light rainfalls, a feat practically impossible to achieve previously. The E-band links are, however, substantially more affected by errors related to variable drop size distribution. Water vapor retrieval might be possible from long E-band microwave links, nevertheless, the efficient separation of gaseous attenuation from other signal losses will be challenging in practice.

1 Introduction

Electromagnetic (EM) waves in the microwave region are attenuated by water vapor, oxygen, fog, or raindrops. Measurements of microwave attenuation at different frequency bands thus represent an invaluable source of information regarding the atmosphere. Passive and active microwave systems have become an integral part of Earth observing satellites, terrestrial remote sensing systems, and complete remote sensing methods in other spectral regions (Woodhouse, 2017). The microwave region is, however, also increasingly utilized in communication systems allowing for new possibilities to observe atmosphere with unintentional (opportunistic) sensing. Commercial microwave links (CMLs) are an excellent example of a communication system capable of providing close-to-ground observations of the atmosphere. CMLs are point-to-point line-of-sight radio connections widely used in mobile phone backhaul for connecting hops of different lengths typically ranging from tens of

meters to several kilometers. There were about 4 million CMLs operated worldwide within cellular backhaul in 2016 (Ericsson, 2016) and about 5 million in 2018 (Ericsson, 2018). Most of these CMLs operate at frequencies between 15 and 40 GHz (Ericsson, 2016, 2018) where raindrops and, to a lesser extent, water vapor represent a significant source of attenuation (Atlas and Ulbrich, 1977; Liebe et al., 1993). Information on the attenuation of any CML within ~~(~~countrywide~~)~~ networks is virtually accessible in real-time with a delay of several seconds from a remote location, typically a network operation center (Chwala et al., 2016) creating an appealing opportunistic sensing system capable of providing close-to-ground observations of rainfall intensity (Leijnse et al., 2007; Messer et al., 2006) and water vapor density (David et al., 2009).

CML rainfall retrieval methods developed over the last decade have been predominantly designed and tested for frequency bands between 15 and 40 GHz (Chwala and Kunstmann, 2019). Attenuation caused by raindrops is, in this frequency region, almost linearly related to rainfall intensity and does not strongly depend on drop size distribution (DSD) (Berne and Uijlenhoet, 2007). Water vapor retrieval has been proposed for CMLs operating around 22 GHz (David et al., 2009) where there is a resonance line of water vapor. Increasing demands on data transfers force operators to utilize higher frequency spectra and a new generation of E-band CMLs, operating at the 71 - 86 GHz frequency band, is gradually modernizing cellular backhaul networks, especially in cities where they often replace older devices. The share of E-band CMLs in mobile phone backhaul has already reached 20 %, *e.g.,* in Poland and the Czech Republic, and it is expected to grow in other countries as E-band CMLs are considered an essential part of new 5G networks (Ericsson, 2019).

E-band CMLs should be, according to recommendations for designing CMLs ~~(ITU-R P.838-3, 2005)~~(ITU-R, 2005), more sensitive to rainfall, nevertheless, the relation between rainfall intensity and attenuation is not linear. Furthermore, E-band radio waves have two to four time's shorter wave lengths and the ~~scattering~~extinction efficiency (resonance peak) is highest for smaller raindrops. The attenuation-rainfall relation is, thus, more sensitive to drop size distribution, which has been already demonstrated in several propagation experiments, *e.g.,* by ~~(~~Hansryd et al., (2010~~;~~) or Luini et al~~.,~~. (2018). Radiowave propagation at an E-band is also more sensitive to water vapor, which poses a challenge when separating rainfall-induced attenuation from other sources of attenuation. On the other hand, the sensitivity to water vapor might also enable its detection or even monitoring.

This manuscript provides the first evaluation of E-band CMLs as rainfall and water vapor sensors. The capabilities of E-band CMLs for weather monitoring are theoretically evaluated and demonstrated on attenuation data retrieved between August and December 2018 from a six E-band CML operated within cellular backhaul of a commercial provider in Prague (T-Mobile, CZ). The ultimate goal of this investigation is to provide an overview of the challenges and opportunities related to atmospheric observations with E-band CMLs. Section 2 of the manuscript summarizes based upon previous works the principles behind retrieving atmospheric variables from CML observations, Section 3 describes the methodology and datasets used in this manuscript for the ~~CML~~ assessment of E-band CMLs, Section 4 presents the results of the case study and evaluates the effect of DSD on the attenuation-rainfall relation. The results are further interpreted and discussed in Section 5 followed by the conclusions which are presented in Section 6.

2 Retrieving atmospheric variables from CMLs

2.1 Components of total observed loss

Standard CMLs are monitored for transmitted ~~(~~*tx* (dBm) and received ~~(~~*rx* (dBm) signal power and the difference between *tx* and *rx* is the total observed loss ~~(~~L_t (dB) which can be separated into several components:

$$L_t = L_{bf} + L_m + L_{tc} + L_{rc} - G_t - G_r, \quad (1)$$

where L_{bf} (dB) is free space loss, L_m (dB) are losses in the medium, L_{tc} (dB) and L_{rc} (dB) are losses at the transmitting and receiving antennas, and G_t (dB) and G_r (dB) are antenna directive gains (Internationale Fernmelde-Union, 2009). Free space loss L_{bf} is uniquely defined by the distance d (m) between the transmitter and receiver, and by wavelength~~,~~ λ (m):

$$L_{bf} = 20\left(\frac{4\pi d}{\lambda}\right) \quad (2)$$

The sum of antenna losses and gains is given by their hardware and includes interference with the environment close to antennas as antenna loss can change, *e.g.*, due to the wetness of antenna radomes. The propagation mechanisms influencing loss in the medium ~~(~~L_m~~)~~ consist of attenuation due to atmospheric gases including water vapor, which is usually not exceeding 1.5 dB km^{-1} (section 2.2), attenuation due to precipitation, which can reach several tens of dB km^{-1} (section 2.3), attenuation due to obstacles in the wave path, and diffraction losses causing bending of the direct wave towards the ground. Total loss can also be influenced by so-called multipath interference occurring due to the constructive or destructive phase summation of the signal at the receiving antenna during the atmospheric multipath propagation conditions (Valtr et al., 2011).

The separation of attenuation due to rainfall~~, resp.~~ and due to water vapor from other sources of attenuation, is possible to some extent, but, firstly, dry and wet weather periods need to be identified (Overeem et al., 2011; Schleiss and Berne, 2010). Attenuation during dry weather is assumed to be a baseline, and the difference between dry and wet weather attenuation is then attributed to rainfall. Fluctuations in the baseline during dry weather can be attributed to water vapor, nevertheless, they can also be caused by temperature changes, hardware instability, etc.

The correct estimation of raindrop path attenuation and water vapor attenuation also requires the separation of additional attenuation caused by antenna radome wetting, so-called wet antenna attenuation (WAA) (section 2.4). This is especially important for shorter CMLs which are attenuated by raindrops along the short path and the relative importance of WAA contribution is significant.

2.42 Attenuation by atmospheric gasses

Attenuation by atmospheric gasses is caused predominantly by the interaction of an EM wave with molecules of water and oxygen. The evaluation of gas attenuation, as described in ~~(ITU-R P.676-11, 2016)~~ ITU-R (2019) and originally in Liebe et al. (1993) ~~and originally in (Liebe et al., 1993)~~, is based on the concept of the complex refractive index. In a medium with complex refractive index n, the intensity of EM wave I (Wm^{-2}) is attenuated at distance x (m) as:

$$I(x) = I(0)\, exp(-2\kappa\, Im(n)\, x), \qquad (7\underline{3})$$

where $\kappa = 2\pi f / c$ (m) is a vacuum wave number ~~(m),~~ c (m s^{-1}) speed of light and $Im(n)$ denotes the imaginary part of n. After introducing complex refractivity $N = (n\text{-}1)10^6$, the specific attenuation k (~~dBkm~~dB km^{-1}) is obtained as:

$$k = 10\, log_{10}\left(\frac{I(0)}{I(1)}\right) = 0.1819\, f\, Im(N), \qquad (8\underline{4})$$

where f (GHz) is the EM wave frequency.

~~In the model (Liebe et al., 1993), total complex refractivity N_t is divided into dispersive and nondispersive parts: $N_t = N_0 + N(f)$. Nondispersive part N_0 is real and does not contribute to attenuation. The dispersive part is given as $N(f) = N_L + N_d + N_c$, where N_L is the contribution of spectral lines of oxygen and water, N_d is from the dry air non-resonant spectrum and N_c is from the water vapor continuum. The key term N_L is determined as a sum of 44 and 35 spectral lines of oxygen and water respectively. The shape and amplitude of the spectral lines depend on temperature, water vapor content and atmospheric pressure.~~

~~Figure 2~~The attenuation due to water vapor is in here defined as the difference between wet-air and dry-air attenuation under the same moist-air pressure and temperature. Thus also effect of water vapor on dry-air attenuation is considered (ITU-R, 2019): First, dry-air pressure decreases during humid conditions (under the assumption of constant moist-air pressure) and second, partial water pressure affects the rate of collisions between the molecules (pressure broadening). Figure 1 shows specific attenuation by water vapor and dry air. Attenuation due to water vapor increases as the frequency increases, with the exception of the peak around 22 GHz and the depression around 60 GHz (Fig. ~~2a~~1a). The sensitivity of water vapor attenuation to temperature and air pressure monotonically increases as the frequency increases. The temperature and pressure also influence dry-air attenuation, especially at frequencies around 60 GHz (Fig. ~~2b~~1b).

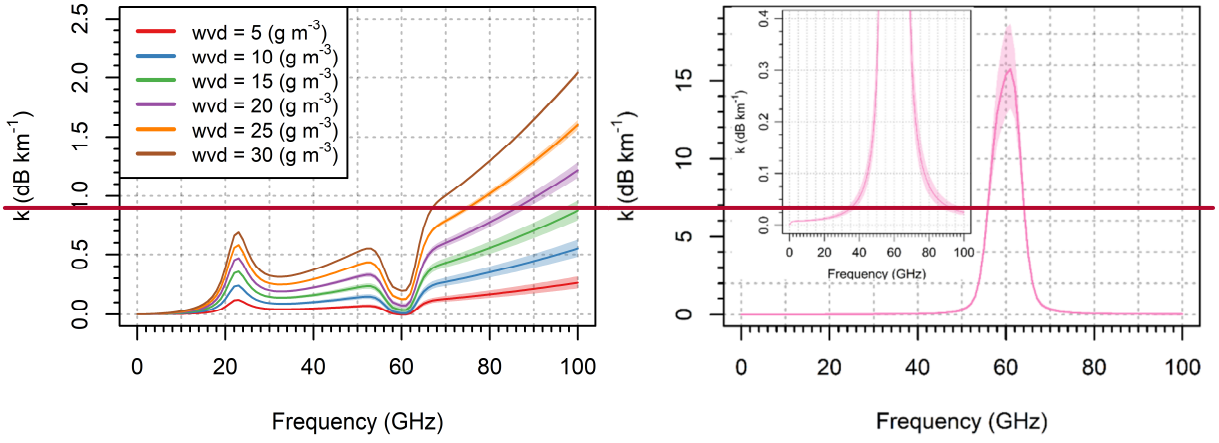

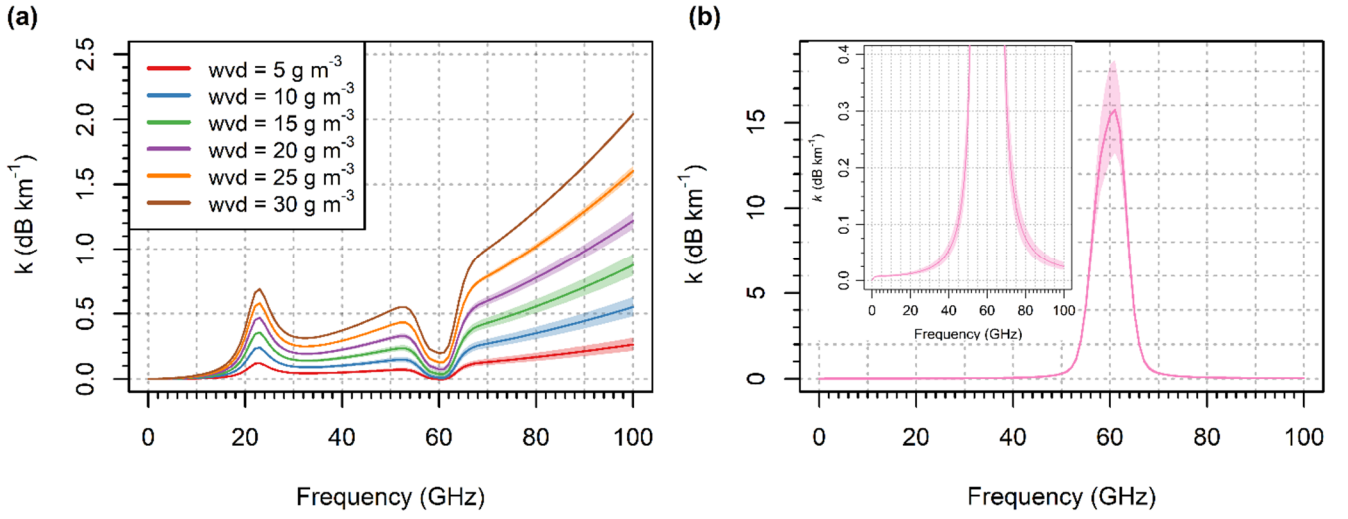

Figure ~~2~~1: (a) Attenuation of EM by water vapor for frequencies 0 to 100 GHz. The relation is shown for different water vapor densities (wvd) for temperatures -10° to +30° C and pressure 1000 to 1030 hPa (colored bands). (b) Dry air attenuation of EM for temperatures -10° to +30° C and pressure 1000 to 1030 hPa (total spread represented by colored ~~band~~bands), inset: a detailed view of the lower attenuations.

2.3 Relation between raindrop path attenuation and rainfall intensity

Attenuation of a direct EM wave due to raindrops can be precisely calculated using the scattering theory. Attenuation caused by a single raindrop is determined by the wavelength, refractive index of water, and shape parameters of the raindrop. The extinction cross section C_{ext}, (cm^2) which can be calculated using the T-matrix method (Mishchenko and Travis, 1998), characterizes the scattering and absorption properties of each raindrop for a given frequency and polarization. The number of drops in the unit volume per drop diameter interval $N(D)$ (m^{-3} mm^{-1}) is relatively small for natural ~~showers~~rainfalls. Therefore, the contribution of scattered secondary EM waves radiated from particles to the incident field of the other particles is negligible. The specific raindrop path attenuation k (dB km^{-1}) can be thus considered as a sum of attenuations caused by single raindrops of diameter D (mm) and can be expressed in integral form:

$$k(f) = 4.343 \times 10^3 \int_{D_{min}}^{D_{max}} C_{ext}(D, f) N(D)\, dD, \quad (~~2~~5)$$

The $N(D)$ also determines rainfall intensity R (mm h^{-1}):

$$R = 0.6\,\pi\, 10^{-3} \int_{D_{min}}^{D_{max}} v(D)\, D^3 N(D)\, dD, \quad (~~3~~6)$$

where $v(D)$ (m s^{-1}) is the terminal velocity of raindrops given by their diameters. As both specific attenuation and rainfall intensity are moments of drop size distribution (DSD~~)~~), the relation between attenuation and rainfall intensity can be approximated by a power-law:

$$k = a\, R^b\,, \quad (~~4~~7)$$

where a (mm^{-b} ~~h~~h^{b} dB km^{-b1}) and b (-) are empirical parameters dependent on frequency, polarization, and DSD. When estimating rainfall from observed attenuation, Eq. ~~4~~(7) can be reformulated to:

$$R = \alpha\, k^{\beta}\,, \qquad (5\text{~~8~~})$$

where α (mm h^{-1} dB$^{-\beta}$ ~~dB$^{-\beta}$ km~~km$^{\beta}$) = $a^{-1/b}$ and β (-) = b^{-1}.

The model (~~4~~7) resp. (~~5~~8) approximates the attenuation-rainfall relation well at frequencies around 30 GHz, nonetheless, errors increase for both lower and higher frequencies due to variable DSD (Berne and Uijlenhoet, 2007). Berne and Uijlenhoet (2007), however, investigated sensitivity to DSD only for the frequency region of 5-50 GHz. A detailed evaluation of the attenuation-rainfall model for the E-band has not been reported, yet higher sensitivity of E-band CMLs to DSD has been demonstrated during several propagation experiments (Hansryd et al., 2010; Luini et al., 2018). Furthermore, different sensitivities of E-band CMLs to DSD, compared to lower frequencies, is also ~~apparent~~obvious from their ~~scattering~~extinction efficiency ~~(Q_{ext})~~:

$$Q_{ext} = \frac{C_{ext}}{\sigma_{geo}}, \qquad (6\text{~~9~~})$$

where C_{ext} (cm^2) and σ_{geo} (cm^2) are extinction resp. geometric cross-sections~~.~~ of a raindrop. The ~~scattering~~extinction efficiency ~~(Fig. 1)~~Q_{ext} of EM waves at the E-band is the highest for smaller raindrops~~,~~ (Fig. 2), which is characteristic for stratiform rainfalls, whereas larger raindrops characteristic for convective rainfalls (section 3.4) contribute relatively less to the total attenuation.

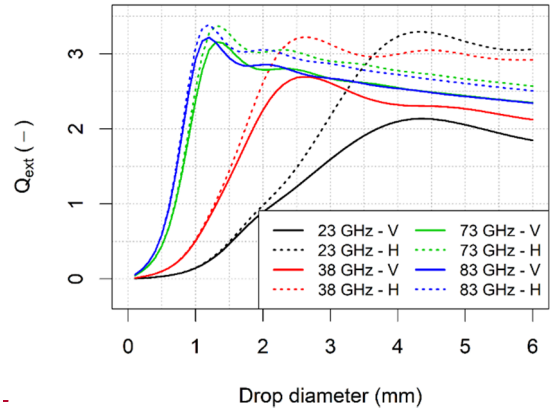

Figure ~~1: Scattering~~2: Extinction efficiency of plane waves at different frequencies and polarizations (H – horizontal, V – vertical).

2.~~2~~4 Wet antenna attenuation

Wet antenna attenuation (WAA) is caused by a water layer forming on antenna radomes during rainfall events or dew occurrence. ~~Modelling~~Modeling WAA is challenging as the formation of water film on antennas is a complex process dependent on rainfall intensity, wind direction and velocity, or air and rain temperature, as well as on antenna radome hydrophobic properties. On the other hand, WAA represents a substantial part of total attenuation (Fencl et al., 2019),

especially by shorter CMLs, and its identification and separation from attenuation caused by raindrops along a CML path is crucial when obtaining reliable rainfall estimates.

Most of the models, specifically suggested for microwave link rainfall retrieval, are empirical and designed for lower frequencies (Minda and Nakamura, 2005; Overeem et al., 2011; Schleiss et al., 2013). However, the semi-empirical model suggested by Leijnse et al. (2008) enables WAA for an arbitrary frequency to be calculated. The Leijnse model assumes a layer of water with constant thickness which is ~~then~~ assumed to be power-law related to rainfall intensity. The parameters of this relation need to be optimized. According to the Leijnse model, WAA typical of E-band CML frequencies is about two times higher than ~~for~~of 38 GHz. Hong et al. (2017), however, showed on 72 and 84 GHz microwave links that WAA depends highly on specific hardware settings. An antenna without radome experienced WAA of about 7 dB during a spraying experiment with artificial rain. The antenna covered by a radome (which is a typical setting ~~for~~of CMLs) experienced WAA of approx. 2 dB and WAA decreased further to only approx. 0.3 dB when a radome with hydrophobic coating was used. Similarly low values of WAA at E-band CMLs have been reported by Ostrometzky et al. (2018) who observed WAAs of 0.86 ~~+-~~ ± 0.54 dB and 1.07 ~~+-~~ ± 0.75 dB at two 73 GHz CMLs. These values are significantly lower than previously observed WAA at lower frequencies (Fencl et al., 2018; Minda and Nakamura, 2005; Schleiss et al., 2013), although E-band CMLs should be, in theory, more sensitive to WAA (Leijnse et al., 2008). ~~More extensive investigations are, therefore, needed to better understand how WAA affects E-band CMLs.~~

3 Material and Methods

The E-band evaluation concentrates on i) gaseous attenuation and its relation to water vapor density and air temperature, ii) the relation between raindrop attenuation and rainfall intensity, ~~ii~~and iii) processing routines for separating different attenuation components~~, and iii) gaseous attenuation and its relation to water vapor density and air temperature~~. The methodology combines numerical experiments using virtual attenuation time series simulated from weather observations with analyses of CML observations obtained during the dedicated case study.

3.1 Experimental sites and instrumentation

Drop size distribution is obtained from a ~~Parsivel~~PARSIVEL disdrometer (1st generation, manufactured by OTT). Drop counts and fall velocities are recorded over 30 s intervals. The data was collected during the CoMMon experiment in Duebendorf (CH) at site 2, which is described, *e.g.*, in ~~(Wang et al., 2012)~~Wang et al. (2012). We further refer to this dataset as Duebendorf data.

The E-band evaluation case study is performed on six CMLs (Table 1) located in the south-east suburb of Prague (CZ). Five shorter CMLs are located in a residential area with a housing estate. The path of the long CML goes over an area with ~~mixed land use,~~ mostly agricultural~~.~~ land use (Fig. 3). The main node from which all CML paths originate is located on the roof of a 65-m-tall building; the end nodes are about 15 m to 30 m above ground ~~(Fig. 3).~~ All the CMLs operate at an Ericsson

MINILINK platform and were deployed to the site during 2016 and 2017. CMLs have full-duplex configuration with two sub-links operating in one direction at 73–74 GHz and in the second direction at 83–84 GHz with a duplex separation of 10 GHz. Transmitted signal power ~~(~~*tx*~~)~~ and received signal power ~~(~~*rx*~~)~~ are collected with custom-made server-sided software which polls selected CMLs using SNMP protocol and stores records into a PostgreSQL database. The sampling time step is approx. 10 s. The resolution of a *tx* and *rx* reading is 0.1 ~~dB~~dBm. All devices have automatic transmitted power control (ATPC), *i.e.*, transmitted power is automatically controlled to minimize fluctuations in *rx*. CML data acquisition is described in detail in the *Supplementary material*.

Tipping bucket rain gauges (MR3, METEOSERVIS v.o.s., catch area 500 cm^2, resolution 0.1 mm) have been deployed at four measuring sites. Two rain gauges are located at the end nodes of the long CML, one at ground level close to the CML path about 1.5 km from the main network node, and one about 2 km south-west from the main node. The rain gauges at sites 1 and 2 are equipped with temperature and air humidity sensors collecting observations in a 5-min time step. ~~To minimize instrumental errors, all~~All four rain gauges have been regularly maintained (on a monthly basis) and are dynamically calibrated (Humphrey et al., 1997). We further refer to the case study dataset as Prague data (Fencl et al., 2020).

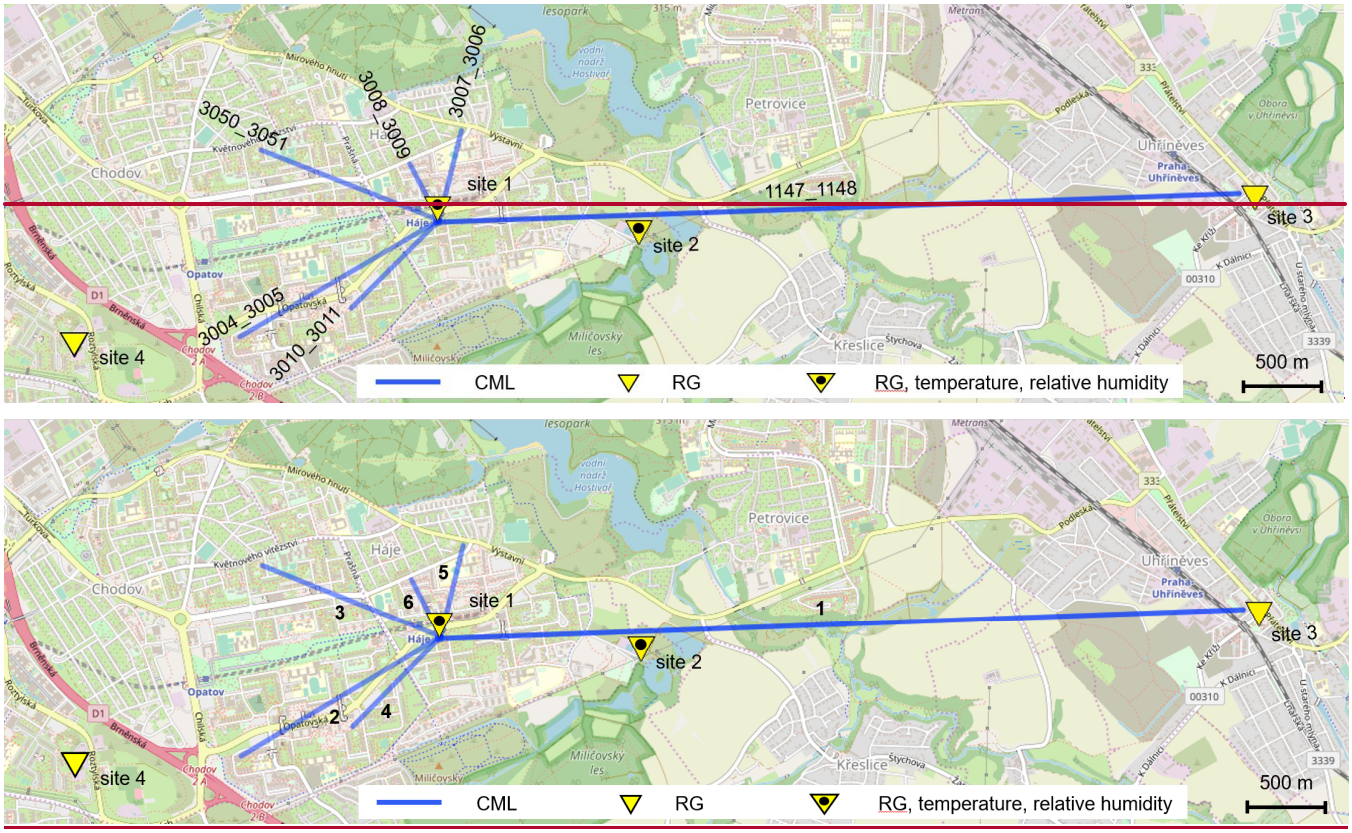

Figure 3: Case study area Prague-Haje, CZ. Two of the rain gauges are equipped with air humidity and temperature probes. ©OpenStreetMap contributors.

Table 1: CML characteristics in Prague-Haje, CZ. The suffixes A and B denote first, resp. second end node, and suffixes AB"a" and BA "b" the direction from A to B resp. B to A.

ID	LonA (deg)	LatA (deg)	LonB (deg)	LatB (deg)	FreqABFreq_a (GHz)	FreqBAFreq_b (GHz)	PolABPol_a	PolBAPol_b	Length (m)
1147_11481	14.52952 90	50.0301	14.59759 70	50.0317	73.5	83.5	V	V	4866
3007_30062	14.53152 91	50.03520 302	14.52915 122	50.03020 237	73.75	83.75	V	V	5731409
3008_3093	14.5291	50.0302	14.52665 140	50.03330 341	73.2572.7 5	83.2582.7 5	HV	HV	3891164
3050_30514	14.5291	50.0302	14.51452 16	50.03410 253	72.7574.2 5	82.7584.2 5	VH	VH	1164765
3004_30055	14.52915 310	50.03020 352	14.51225 291	50.02370 302	73.75	83.75	V	V	1409573
3010_30116	14.5291	50.0302	14.52165 266	50.02530 333	7473.25	8483.25	H	H	765389

3.2 Experimental data

Experimental periods: Duebendorf data span from March 2011 to April 2012. Prague data span from 20th August to 16th December 2018. The rainfall observations are, due to technical problems available from 28th October to 16th December 2018. The periods for evaluating rainfall retrieval and for evaluating the effect of humidity and temperature fluctuations on gaseous attenuation are, therefore, different.

Duebendorf data: The disdrometer data is quality-checked and suspicious records are excluded using filters described in (Jaffrain and Berne, 2010)Jaffrain and Berne (2010). Moreover, only records classified by the disdrometer as rainfall (at least from 90 %) are used for further analysis; hail events are excluded. The data which pass the quality check are aggregated to a 1-min temporal resolution using averaging.

Prague data: Total loss is calculated for each CML as the difference between transmitted and received signal powers. The total loss data is aggregated using averaging to a 1-min temporal resolution.

Rain-gauge data are separated into rainfall events. An event is defined as a period with intervals between consecutive rain gauge tips shorter than one hour. The rainfall events with rainfall heightdepth lower than 1 mm are excluded from the

evaluation. Furthermore, events during which the temperature dropped below 2° C were also excluded from the evaluation to limit the performance assessment to liquid precipitation only. This results in a set of five events (see Table 2) representing, in terms of total depth, 81 % of all the precipitation during the experimental period. Rainfall data are aggregated by averaging to a 15-min temporal resolution to limit uncertainties due to rain gauge quantization and uncertainties related to uncaptured rainfall spatial variability. The 15-minute rainfall intensities are, for all four rain gauges, highly correlated (r = 0.88–0.96). The cumulative rainfall observed by the rain gauges is also in very good agreement and differs from the mean rainfall only by 1–3- %.

The air temperature and relative humidity data (5-min temporal resolution) ~~is~~are not further processed. The correlation coefficient between temperature observations is 0.95 and between humidity observations 0.86. In general, observations on the roof of the ~~70~~65-m-tall building (site 1) have slightly lower variability than close-to-ground observations (site 2). The discrepancies are especially pronounced during transient conditions in the morning ~~hours~~.

Table 2: Rainfall events used for the evaluation of CML rainfall retrieval

Event start	Duration (min)	~~Height~~ Depth (mm)	R_{max} (mm h^{-1})
2018-10-28 01:10	1218	21.0	4.4
2018-11-02 19:14	500	5.1	2.5
2018-11-24 09:46	176	1.9	1.7
2018-12-03 05:00	158	1.8	2.6
2018-12-03 22:03	210	4.9	3.0

3.3 Gaseous attenuation

The effect of temperature and air humidity on total CML attenuation is estimated theoretically from observed air temperature and relative humidity (see section 2.42) and compared to the real CML data obtained during the case study~~.~~ from the long CML (ID 1). Atmospheric pressure was not measured and is assumed to be constant ~~at a~~ corresponding to average sea-level ~~of 1013.25 hPa. Variations in atmospheric~~ pressure. Atmospheric pressure changes related to weather conditions have, however, an almost negligible effect on theoretical attenuation ~~(the results of the sensitivity analysis are not shown here).~~(ITU-R, 2019). The temperature and air humidity used in the analyses are averages from the observations at two locations along the CML path. Gaseous attenuation is estimated for the period from 20th August to 16th December 2018 and only considers dry weather, *i.e.,* periods without rainfall and dew occurrences (events causing the tipping of at least one of the rain gauges). A safety window of 6 h was set before and after each event with an event considered to start with the first tip of any rain gauge and ending with the last tip.

The theoretical attenuation derived from air temperature and relative humidity observations is then compared to the observed attenuation of the long CML. To enable a comparison, the observed attenuation is also aggregated to a 5-min time step corresponding to the time step of temperature and humidity observations, resp. theoretical attenuation. Furthermore, the constant baseline is subtracted from the observed attenuation time series. The constant baseline is set separately for each sub-link (73.5 GHz and 83.5 GHz), such as the median attenuation obtained after the baseline separation corresponds to the median theoretical attenuation. The median attenuation is calculated considering dry-weather periods only.

~~**Gaseous attenuation:** The effect of air humidity and temperature on attenuation patterns is demonstrated during dry-weather periods on the sub-links belonging to the long CML.~~ The observed attenuation patterns are compared to the theoretical patterns calculated from temperature and air humidity observations assuming constant atmospheric pressure ~~1013.25 hPa~~at sea level. The agreement between theoretical and observed attenuation is quantified in terms of correlations and the magnitude of their amplitudes. In addition, seasonal drift is demonstrated on time series smoothed by a moving average with a window size of one week.

Table 3: Empirical parameters of convective and stratiform rainfall for DSD reconstruction as observed by Fujiwara (1965) and re-parameterized by Ulbrich~~,~~ (1983).

Type	N_0 (m^{-3} $cm^{-1-\mu}$)	μ (-)	ε ($h^{-\delta}$)	δ (-)
Convective (thunderstorm)	$7.05\ 10^4$	0.4	0.118	0.20
Widespread or stratiform	$1.96\ 10^5$	0.18	0.082	0.21

Note: N_0 ($m^{-3}cm^{-1-\mu}$) and μ (-) are parameters of semi-empirical gamma distribution function, ε ($h^{-\delta}$) and δ (-) are scaling parameters of this function.

3.~~3~~4 Sensitivity of the k-R model to drop size distribution

The analysis of the k-R model (~~5~~Eq. 8) with respect to DSD is based on fitting Eq. ~~3~~(8) on attenuation and rainfall intensities obtained from Eq. ~~1~~(5) and ~~2.~~(6). c First, the sensitivity of the k-R model parameters (8) to the type of rainfall (stratiform vs. convective) is investigated on theoretical DSD and secondly on real DSD from the Duebendorf dataset.

Investigation of theoretical DSD: The number of drops N with diameter D is modeled using the gamma distribution function scaled to rainfall intensity (Ulbrich, 1983). ~~(Ulbrich, 1983).~~Ulbrich (1983). The empirical parameters needed for the reconstruction of $N(D)$ for stratiform and convective rainfall are in Table 3. The distribution functions for two different rainfall intensities are shown in Fig. 4.

$N(D)$ is calculated for a sequence of reference rainfall intensities from 0 to 50 mm h^{-1} with an increment of 0.1 mm h^{-1} for both types of rainfalls. Specific attenuations corresponding to a given intensity and rainfall type are then calculated according to Eq. (~~2~~5). Specific attenuations are calculated for 73.5 and 83.5 GHz, vertical polarization, *i.e.*, frequencies of the sub-links

belonging to the long CML in the Prague data. These frequencies are approximately in the middle of the frequency bands of 71–76 GHz and 81–86 GHz allocated for E-band fixed wireless services and, thus, representative for all E-band CMLs.

The k-R model (~~5~~Eq. 8) is fitted separately for each frequency and rainfall type by minimizing the sum of squared residuals between reference rainfall intensities (Eq. 6) and rainfall intensities estimated by the model using a specific attenuation obtained by Eq. (~~2~~5).

Investigation of Duebendorf DSD data: The effect of DSD on the k-R power-law approximation is further tested on DSD data (~~Deubendorf~~Duebendorf) and its influence on rainfall estimation accuracy is quantified. The procedure is analogous to the analysis of the theoretical DSD. However, rainfall intensities and specific attenuations are calculated from the observed DSD. The rainfall records are classified into two types according to the mass-weighted drop diameter D_m (~~m~~mm), which is the ratio between the fourth and third DSD moments:

$$D_m = \frac{\int_{D_{min}}^{D_{max}} N(D) D^4 dD}{\int_{D_{min}}^{D_{max}} N(D) D^3 dD} \quad , \qquad (~~9~~10)$$

The mass-weighted diameter D_m is a common descriptor of the center of a probability density function $f(D)$ characterizing DSD, thus the D_m-based classification resembles the classification on convective and stratiform rainfalls (Jaffrain and Berne, 2012). The mass-weighted diameter can be approximately related to the rainfall intensity by a power-law function:

$$\widehat{D_m} = c\, R^d, \qquad (~~10~~11)$$

where R (mm h^{-1}) is rainfall intensity and c (h^{-d} mm$^{1/d}$) and d (-) are empirical parameters. Such an approximation results in perfect fits for stratiform and convective rainfall types when applied to theoretical DSD (Fig. 4b). The approximation (~~10~~Eq. 11) is~~, therefore,~~ used to calculate ~~rainfall intensity dependent on the~~ threshold for classifying ~~rainfalls~~disdrometer records as convective or stratiform. The threshold is dependent on rainfall intensity. Parameters c and d are estimated by fitting Eq. (~~10~~11) to D_m as derived from real disdrometer data ~~usage by~~using Eq. ~~(9).~~ (10).

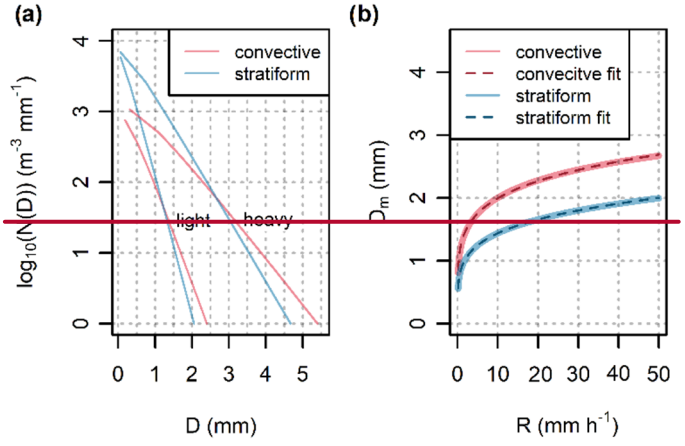

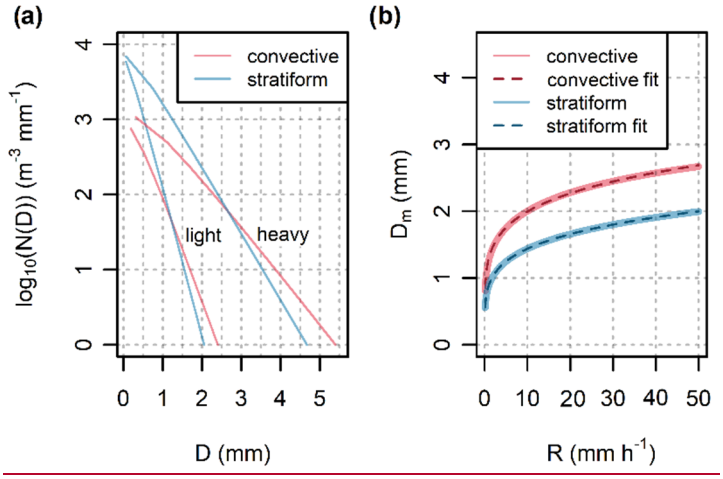

Figure 4: (a) Theoretical DSD for light (1 mm h^{-1}) and heavy (50 mm h^{-1}) convective and stratiform rainfall, and (b) the power-law relation between mass weighted diameter D_m and rainfall intensity for the same rainfall types. Gamma distribution functions with parameters corresponding to storms reported by ~~(Fujiwara, 1965)~~ Fujiwara (1965) are used.

Performance evaluation: The performance of k-R power-law approximation is evaluated by comparing rainfall intensities obtained directly from DSD (~~3~~Eq. 6) to rainfall intensities estimated from the k-R model (~~5~~Eq. 8). Virtual specific attenuations derived from DSD (~~2~~Eq. 5) for two different frequencies are used as inputs to the k-R model.

The performance is evaluated for three model settings: i) the k-R model with a single set of parameters obtained by fitting the model to the whole dataset, ii) the k-R model with two sets of parameters for periods with stratiform resp. convective rainfall obtained by fitting the model separately for these two rainfall types, iii) the k-R model with parameters from ITU recommendations ~~(ITU-R P.838-3, 2005).~~(ITU-R, 2005).

The analysis is first ~~performed~~evaluated for the theoretical DSD (theoretical ~~pdfs~~PDFs describing drop size spectra) and secondly, in more detail, for DSD measured by a disdrometer. In the second analysis, the k-R model is evaluated in terms of ~~RMSE (~~root mean square error criterion (RMSE) for the whole dataset and then separately for light ($R \leq 4$ mm h^{-1}), moderate (4 mm h^{-1} < $R \leq 12$ mm h^{-1}) and heavy ($R > 12$ mm h^{-1}) rainfalls. The parameters of the k-R model obtained for Duebendorf data are verified on CML attenuation observations ~~(CML 1147_1448)~~ in Prague data.

3.5 CML rainfall retrieval

Rainfall retrieval is performed for each sub-link separately. First, total observed loss aggregated to a 1-min resolution is quality-checked ~~for hardware-related artifacts~~. Second, total observed loss is aggregated to a 15-min temporal resolution and the baseline is identified and separated. Third, WAA is estimated and, finally, attenuation corrected for WAA is converted to rainfall intensity. Although dry-wet weather classification is not used for rainfall retrieval in this study, it is included in the ~~performance assessment~~*Appendix A* as it might be needed for future studies and applications (see Discussion section).

Quality check: All the time series of total losses are visually inspected to identify obvious hardware related artifacts. In one case (CML ~~3004_3005~~2), the sudden change in the baseline is manually corrected, as automated procedures used for attenuation processing are not designed to cope with this artifact. Hardware-related artifacts are in more detail presented in *Appendix B.*

Baseline identification: Background attenuation, the so-called baseline, is needed to identify rainfall induced attenuation and is estimated as a moving median with a centered window having a size of one week applied on time series of total losses averaged over ~~hourly~~15-minute intervals. A one-week window size seems to be appropriate for the climate of the Czech Republic as it covers a period with more than half of the records belonging to dry weather. On the other hand, it is sufficiently short to ~~capture~~ reliably capture long-term baseline drifts related to the instability of the CML hardware, or gaseous attenuation.

Wet antenna attenuation: WAA during rainfall is estimated by comparing attenuations as observed by sub-links of different path lengths. WAA quantification assumes spatially uniform rainfall under which specific attenuations $k_1, k_2, \ldots, k_n$ (dB km^{-1}) of the sub-links 1, *2, …, n* operating at the same frequency band in the same area should be identical:

$$k_1 = \frac{A_1 - Aw_1}{l_1} \approx k_2 = \frac{A_2 - Aw_2}{l_2} \approx \cdots \approx k_n = \frac{A_n - Aw_n}{l_n}, \quad (~~11~~12)$$

where A (dB) is rainfall-induced attenuations, *i.e.*, the difference between total observed loss ~~(L_T)~~ and the baseline, Aw (dB) is wet antenna attenuation and l (km) is CML (sub-link) length. Assuming correct baseline identification and the same Aw for all CMLs, Aw can be directly quantified from any pair of sub-links of different lengths operating at the same frequency. The accuracy of the quantification relies on the fulfillment of the assumptions and the difference between the sub-link lengths. The larger is the length difference between the CMLs, the smaller is the effect of an inaccurate baseline identification or dissimilar Aw within the CML pair. On the other hand, the assumption of spatially uniform rainfall is unlikely to be valid for CMLs covering a large area, *i.e.*, with contrasting lengths.

WAA is quantified at each time step by comparing the attenuation of the short CMLs to the attenuation of the long CML. WAA after rainfall and during dew events is assumed to be equal to the total attenuation.

~~**Wet antenna attenuation:** Wet antenna attenuation during rainy periods is~~ WAA evaluated for ~~shorter~~short CMLs ~~and~~is then related to rainfall intensity in terms of correlation. Wet antenna analysis is performed on attenuation data aggregated to 15 min.

Rainfall estimation: Rainfall is estimated for each sub-link using the k-R power-law model (~~5~~Eq. 8) with ITU parameters and parameters derived from DSD classified as stratiform rains, alternatively. The parameters for stratiform rainfalls are used for its dominance in light and moderate autumn rainfalls in the Czech Republic. The specific attenuation k (dB km^{-1}) used as an input to the k-R model ~~(5)~~ is calculated:

$$k = max\ (\frac{L_t - B - Aw_{const}}{l}, 0), \quad (~~12~~13)$$

where L_t (dB) is the total observed loss, B (dB) is the baseline, Aw_{const} (dB) is constant WAA, and l (km) is the CML, resp. sub-link path length. The constant WAA is estimated separately for 73–74 GHz and 83–84 GHz sub-links as the median of WAA values quantified according to Eq. (~~11~~12).

~~Rainfall retrieval:~~ CML rainfall retrieval performance is evaluated for two sets of k-R model parameters: parameters derived from ITU recommendations and parameters obtained from DSD observations (Duebendorf) classified as stratiform. The CML quantitative precipitation estimates (QPEs) of the long CML are compared to average 15-min rainfall from rain gauges ~~rg~~ at the sites 1, ~~rg~~ 2, and ~~rg~~ 3. The QPEs of the short CMLs are compared to average 15-min rainfall from rain gauges ~~rg~~ at the sites 1, ~~rg~~ 2, and ~~rg~~ 4. The quantitative evaluation focuses on the long CML, which is sufficiently long ~~enough~~ to capture even the light rainfalls dominating the Prague data. The performance of the short CMLs is shown to demonstrate limitations related to the improper baseline and WAA identification which are, especially during light rainfalls, more pronounced by shorter CMLs. The CML QPEs are evaluated over selected rainfall events (Table 2) in terms of correlation, relative error in cumulative rainfall, and ~~root mean square error (~~RMSE~~).~~.

~~**3.6 Performance evaluation**~~

~~**Hardware related artifacts:** Hardware related artifacts are identified (visually) in the time series of total observed losses and described.~~

4 Results

4.1 Gaseous attenuation – effect of air humidity and temperature

Theoretical gaseous attenuation calculated from observed temperatures and relative humidity is highly correlated to water vapor density (r = 0.94–0.97) at both frequencies studied. The fluctuations in temperature affect this relation negligibly. The further evaluation, therefore, concentrates on the comparison of theoretical attenuation to attenuation observed by two sub-links of the long CML ~~1147_1148~~1. To separate gaseous attenuation from other possible attenuations, only periods with no rainfall are evaluated.

Time series of theoretical and observed attenuation are compared in Fig. ~~12~~5 which shows time series of attenuations smoothed by a moving average (one-week window size). The correlation between theoretical and observed attenuation is high for both sub-links (r = 0.82–0.83) and the long-term patterns of observed and theoretical attenuations correspond to each other quite well. Both theoretical and observed attenuations are higher during the summer period (August-September) and gradually decrease during the autumn period (October–December). The difference between mean attenuation levels in August and December is about 1 dB for the 83.5 GHz sub-link compared to only 0.7 dB for the 73.5 GHz sub-link. The theoretical and observed attenuations have similar median values for both frequencies during summer (2.11 resp. 2.12 dB for 73.5 GHz and 2.05 resp. 2.09 dB for 83.5 GHz). The theoretical and observed attenuations during autumn are about 0.3 dB higher for 73.5 GHz, compared to the 83.5 GHz sub-link (1.81 resp. 1.93 dB for 73.5 GHz compared to 1.58 resp. 1.65 dB for 83.5 GHz).

The higher attenuations of the 73.5 GHz sub-link during the autumn period, in comparison to the 83.5 GHz sub-link, can be explained by dry air attenuation. Dry air attenuation of 73.5 GHz is about 0.2 - 0.3 dB higher (depending on temperature) than that of 83.5 GHz. On the other hand, higher frequency bands are more sensitive to water vapor attenuation, which is higher during summer. Different sensitivity to water vapor attenuation also causes more significant seasonal drift in the attenuation of the 83.5 GHz sub-link compared to the 73.5 GHz one.

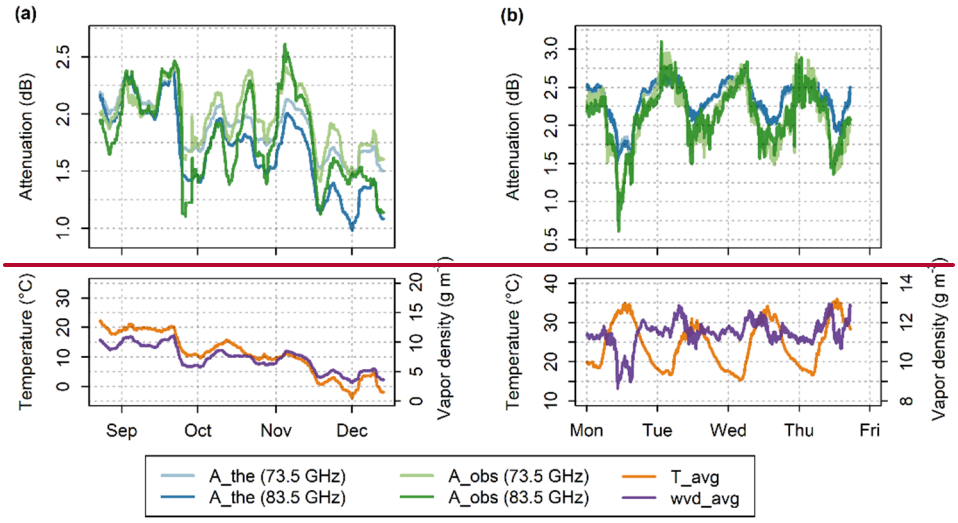

~~**Figure 12: Theoretical and observed attenuation from the 73.5 and 83.5 GHz sub-links of CML 1147_1148 – (a) data over the whole observation period smoothed by a moving average with a window size of one week; (b) 5-min data during four summer days.**~~

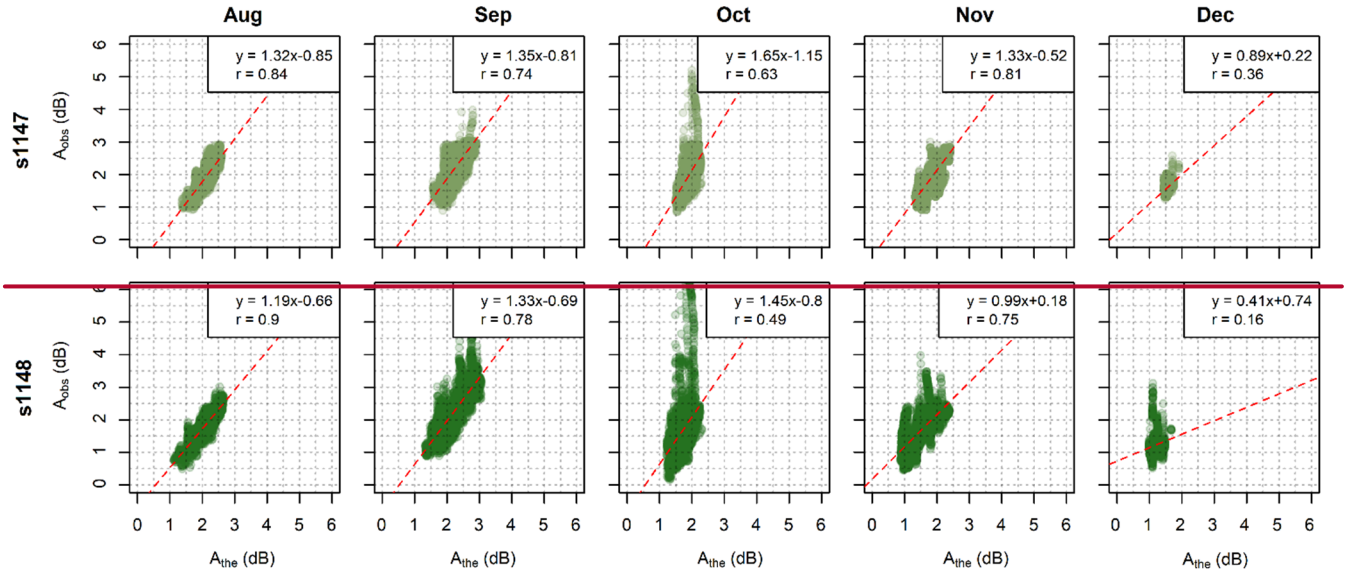

~~**Figure. 13: Comparison of theoretical (x-axis) and observed (y-axis) gas attenuations at the 73.5 and 83.5 GHz sub-links of the CML 1147_1148 for 5-min data. Data are shown separately for each month.**~~

The discrepancies between theoretical and observed attenuations are more pronounced when analyzing data at a 5-min resolution, as demonstrated on the time series of four summer days shown in Fig. ~~12b~~5b. This is because the separation of gaseous attenuation from the other sources of attenuation or hardware related artifacts is challenging in real conditions. Despite these discrepancies, the correlation between theoretical and observed attenuations remains relatively high (r = 0.70–0.72). The theoretical and observed attenuations are highly correlated during ~~the summer period~~August (Fig. ~~13~~6) with the correlation coefficients reaching 0.84 and 0.90 for the 73.5 GHz (1a) resp. 83.5 GHz (1b) sub-link. The correlation is lowest during December (r = 0.36 resp. 0.16).

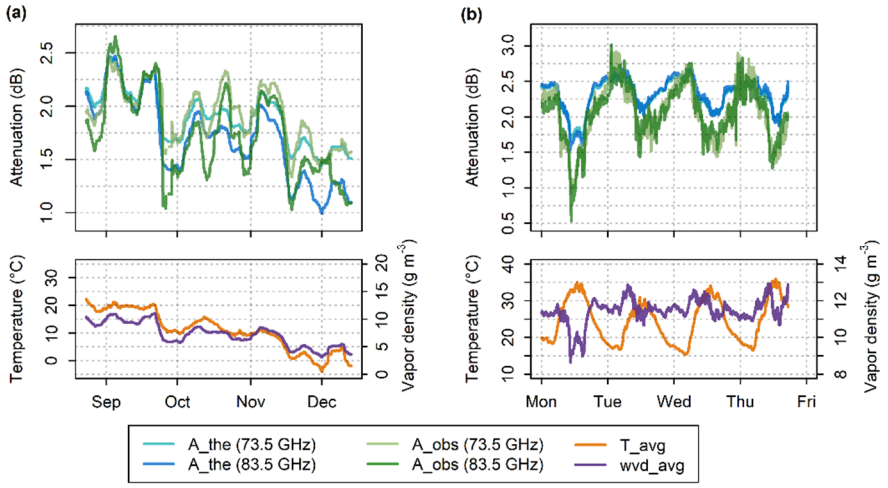

Figure 5: Theoretical and observed attenuation from the 73.5 and 83.5 GHz sub-links of CML 1 – (a) data over the whole observation period smoothed by a moving average with a window size of one week; (b) 5-min data during four summer days.

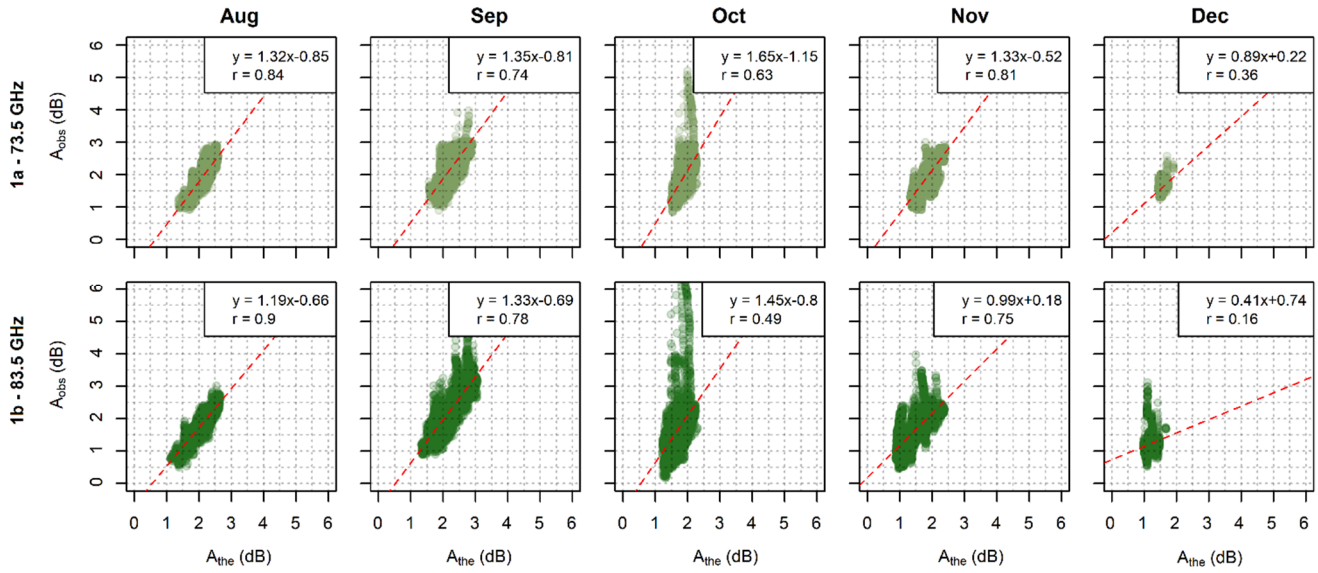

Figure. 6: Comparison of theoretical (x-axis) and observed (y-axis) gas attenuations at the 73.5 and 83.5 GHz sub-links of the CML 1 for 5-min data. Data are shown separately for each month.

4.2 Accuracy of the k-R power-law approximation

Evaluation of theoretical DSD: The relationship between attenuation and rainfall can be, for both frequencies, extremely well approximated by the power-law model, however, the parameters heavily depend on DSD (Fig. ~~9~~7). For example, the specific attenuation 16 dB km^{-1} corresponds to a rainfall intensity of about 30 mm h^{-1} for rainfall with DSD typical for stratiform rainfalls. However, throughout convective rainfall the same specific attenuation would occur for rainfall intensities of about 50 mm h^{-1}. For both frequencies the model ~~uses~~using ITU parameter results between curves fitted to the rainfalls with stratiform resp. convective DSD. However, it is closer to the 'stratiform' curve for lower rainfall intensities and approximates a better 'convective' curve for intensities higher than approx. 10–15 mm h^{-1}. The ITU parameters, therefore, provide a good approximation when no information on precipitation type is available.

Evaluation on ~~DSD data~~ Duebendorf DSD data: Similar power-law fits are obtained when ~~modelling~~modeling attenuation and rainfall from real DSD observations. Here, two types of rainfall are classified based on mass-weighted drop diameter D_m (~~9~~Eq. 10). The fitting of the classification threshold $\widehat{D_m}$ (~~10~~Eq. 11) results in parameters c = 1.29 h^{-d} mm$^{1/d}$ and d = 0.16. The relation between rainfall intensity and theoretical attenuation obtained is shown, together with fitted k-R power-law curves, in Fig. ~~10~~8. The ~~relation between~~spread of rainfall intensity ~~and~~ clearly grows with increasing attenuation ~~is clearly heteroscedastic.~~. The k-R model deficiencies, therefore, increase with increasing rainfall intensity, as can be also seen from the RMSE values (Table 4).

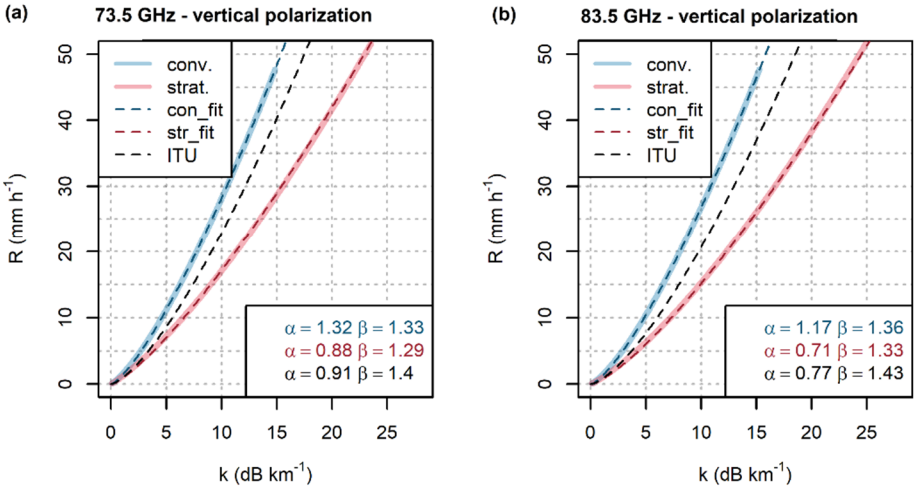

Figure ~~9~~7: Attenuation-rainfall relation for vertically polarized radio waves at (a) frequency 73.5 GHz and (b) 83.5 GHz derived from theoretical DSD corresponding to stratiform and convective rainfall. ~~A k-R model (5) with parameters according to ITU (ITU-R P.838-3, 2005)~~A k-R model (Eq. 8) with parameters according to ITU-R (2005) lies between the curves corresponding to virtual convective and stratiform rainfalls. Parameters of the models are shown ~~in the legends in the lower right-hand corners~~.

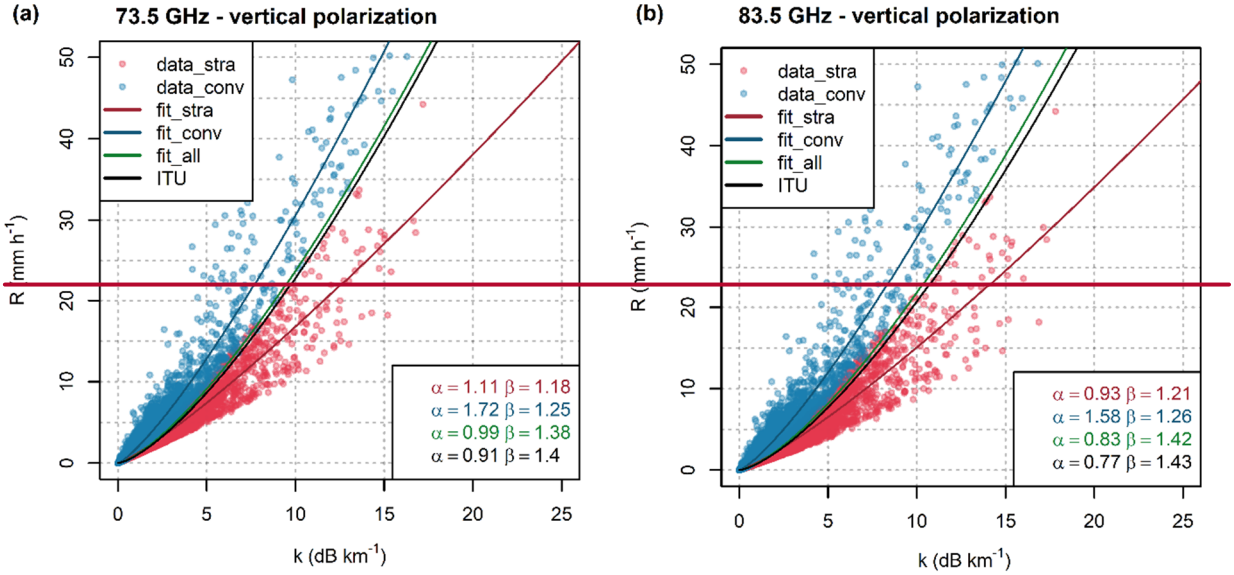

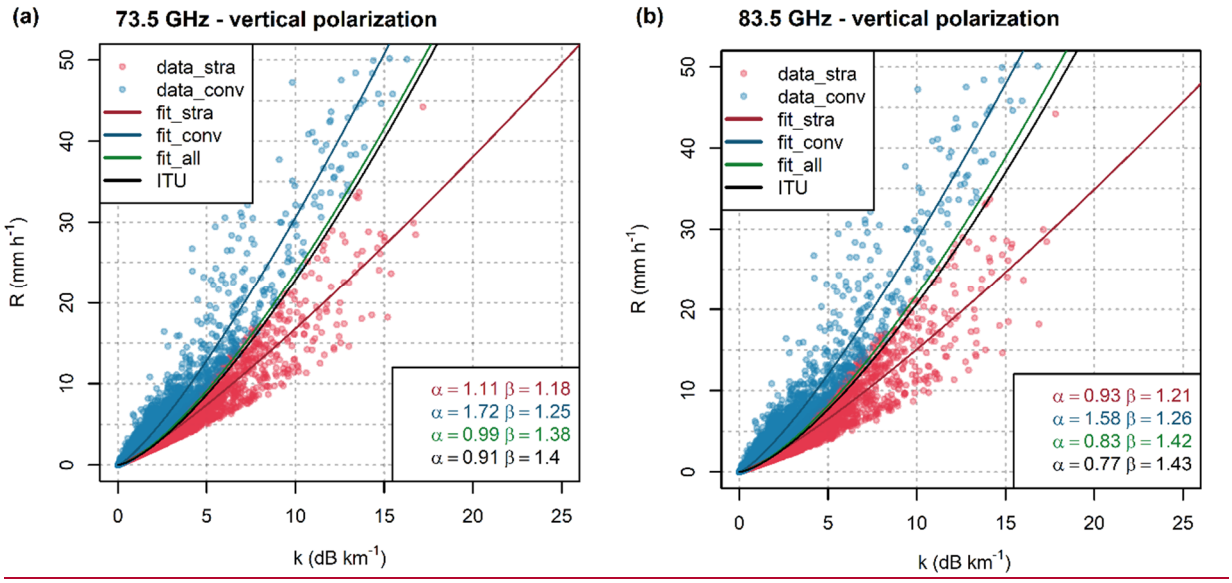

Figure ~~108~~: Relation between specific attenuation and rainfall derived from one year of DSD data for vertically polarized radio waves at (a) frequency 73.5 GHz, and (b) 83.5 GHz. ~~The k-R model (5) with parameters according to ITU (ITU-R P.838-3, 2005)~~The k-R model (Eq. 8) with parameters according to ITU-R (2005) resembles the model optimized for all the records. The curves optimized for convective and stratiform rainfalls differ significantly. Parameters of the models are shown ~~in the legends in the lower right-hand corner~~.

Table 4: RMSE values ~~(mm h^{-1}) calculated for~~measuring differences between observed and simulated rainfall using the k-R model with different parameter sets. The evaluation is provided separately for light, moderate, and heavy rainfall as well as for the whole dataset.

Parameter set	Freq. (GHz)	RMSE (mm h^{-1})			
		~~all~~*All data*	*Light rainfall* $R \leq 4$	*Moderate rainfall* $R = 4$–12	*Heavy rainfall* $R > 12$
Separate fit	73.5	0.67	0.20	1.34	4.75
	83.5	0.73	0.24	1.48	5.08
Joined fit	73.5	1.17	0.43	2.46	8.03
	83.5	1.26	0.41	2.73	8.43
ITU	73.5	1.18	0.41	2.39	8.17
	83.5	1.27	0.45	2.63	8.74

4.3 Wet antenna attenuation

Figure ~~8~~9 presents CML data at a 1-min temporal resolution featuring: i) attenuation during peak rainfall; ii) attenuation during dry spells at night on 3rd Nov. and after ~~a~~the rainfall; and iii) attenuations during dew occurrence on the morning of 4th Nov. Attenuation during peak rainfall is ~~dominated~~markedly influenced by raindrop path attenuation and is proportional to path length~~.~~ (Fig. 9b). In contrast, attenuation both during dry spells and after a rainfall, as well as attenuation during dew occurrences (with the exception of sub-link ~~3009~~6b) is dominated by WAA and, thus, independent of path length. Therefore, the WAA quantification method utilizing different CML path lengths (section 3.5) seems to be conceptually justified.

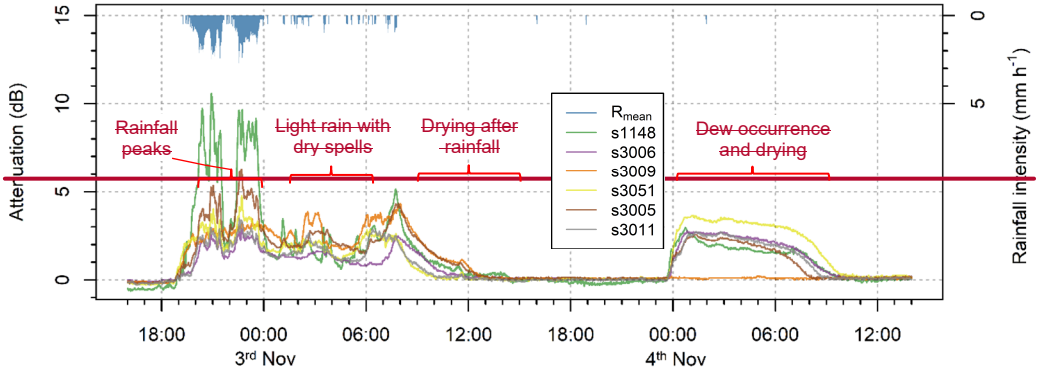

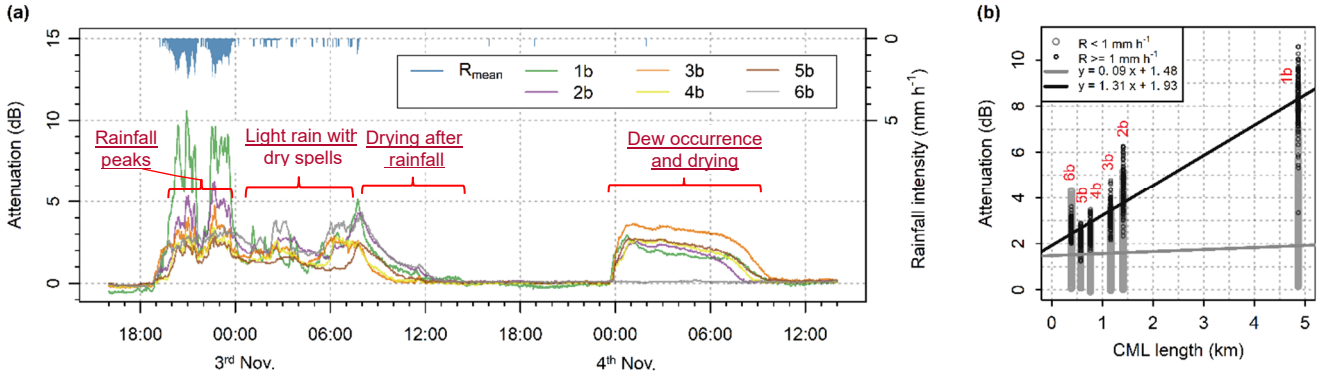

Figure ~~7~~9: (a) Total rainfall-induced attenuation of 83–84 GHz sub-links and mean rainfall intensity from all four rain gauges. Period with peak rainfalls on 2nd Nov ~~form~~. from approx. 19:00 to 00:00, period with light rainfall and dry spells on 3rd Nov ~~form~~. from approx. 00:00 to 05:00, antenna drying period on 3rd Nov. from approx. 08:00 to 14:00, and dew occurrence and subsequent antenna drying on 4th Nov ~~form~~. from approx. 00:00 to 10:00. (b) Total attenuation plotted against path length for 83-84 GHz sub-links with two separate linear fits for intervals with moderate rainfall and intervals with very-light rainfall including dry spells. Period from 19:00 on 2nd Nov. to 14:00 on 3rd Nov. is shown.

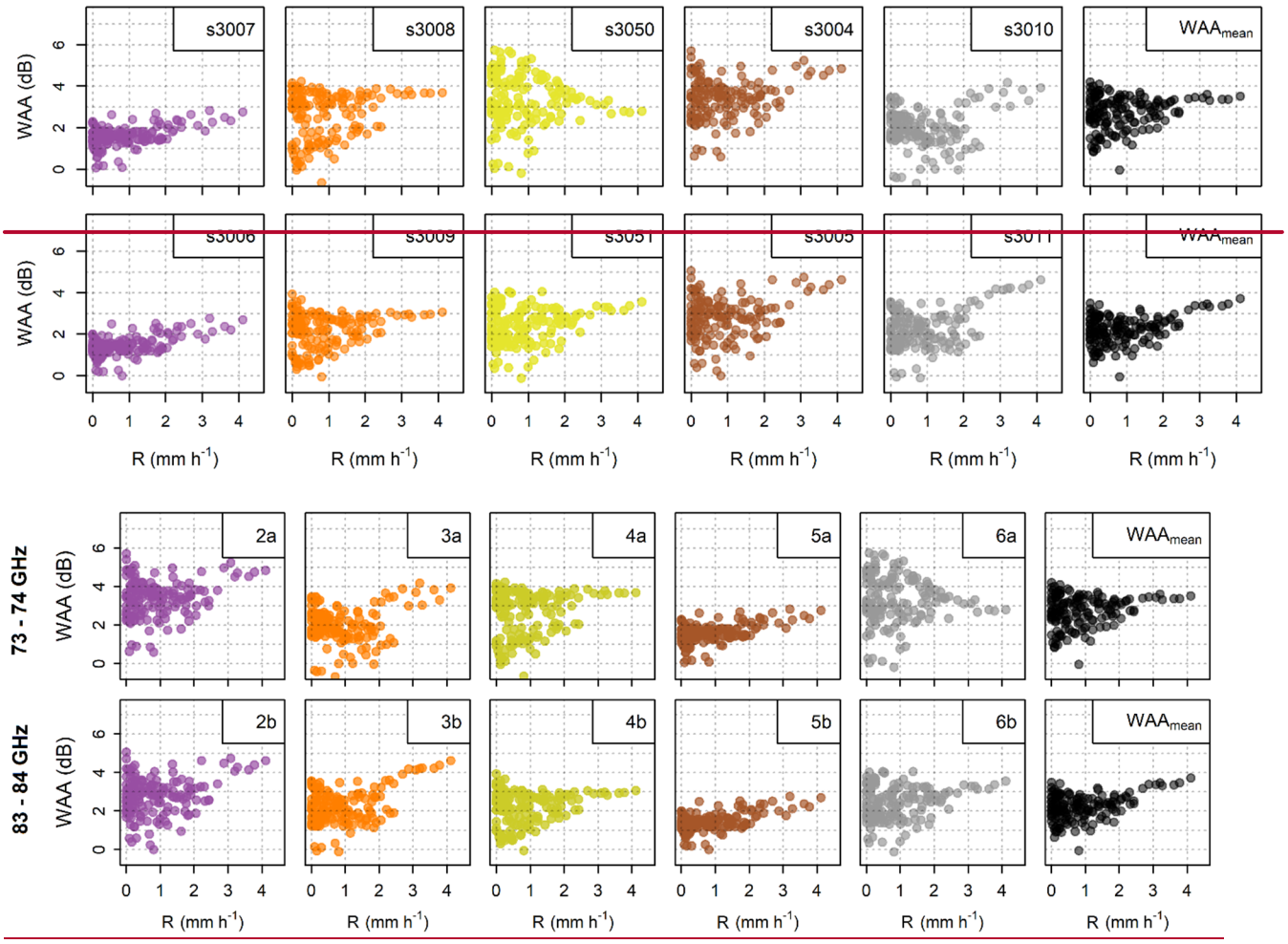

Figure ~~8~~10: Wet antenna attenuation during rainfall estimated from the differential attenuation of short and long CMLs. WAAs for both sub-links (73–74 GHz and 83–84 GHz) are shown for CML 1–5. The panels on the right side show mean WAA for all CMLs.

WAA quantified for each shorter CML and their average is shown in Fig. ~~8~~10 at a 15-min temporal resolution. The correlation to rainfall intensity is weak except for sub-links ~~30086~~6a and ~~30065~~5b with correlation coefficients r = 0.46 and r = 0.53, respectively. Higher rainfall intensities are, in general, associated with high WAA, whereas WAA reaches a wide range of values during lower intensities. WAA averaged over the whole evaluation period is between 1.60–3.47 dB for the 73–74 GHz sub-links and 1.41–2.48 for the 83–84 GHz sub-links. Further, inspection of CML time series reveals that attenuation after rainfall decreases exponentially which is probably due to the drying of the antennas (Fig. ~~7~~9a, 3rd Nov).

WAA also contributes to total attenuation during the occurrence of dew when water condensates on the antenna radomes. Attenuation associated with dew deposition is similar for both frequency bands and reaches up to 4 dB (Fig. ~~7~~9a, 4th Nov morning). These values are higher than ~~attenuation~~WAA caused by rainfall.

4.4 Rainfall estimation

Figure 11 shows QPEs obtained from CMLs using the k-R model with ITU parameters and parameters derived from DSD during rainfalls classified as stratiform. Note that DSD is obtained from the independent Duebendorf dataset. The long CML, in particular the 83.5 GHz sub-link, is capable of capturing even light rainfall intensities reliably. The correlation to rain-gauge observations is excellent ($r \approx 0.96$). However, QPEs derived with ITU parameters tend to underestimate light rainfalls, which also leads to increased RMSE (Table 5). The model with DSD-derived parameters improves performance with respect to all metrics. Sub-link ~~1147~~1a also remains significantly underestimated with DSD-derived parameters. This is due to deficits in the baseline and WAA identification. The underestimation is pronounced especially during very light rainfalls with rainfall intensities under 1 mm h^{-1}, which represent 25 % of total rainfall depth. Shorter CMLs are less sensitive to rainfall along their shorter path and are more affected by deficiencies in the estimated baseline and WAA. Thus, use of DSD parameters does not significantly improve performance of short CMLs. CMLs shorter than 1 km overestimate rainfall intensities more than longer CMLs.

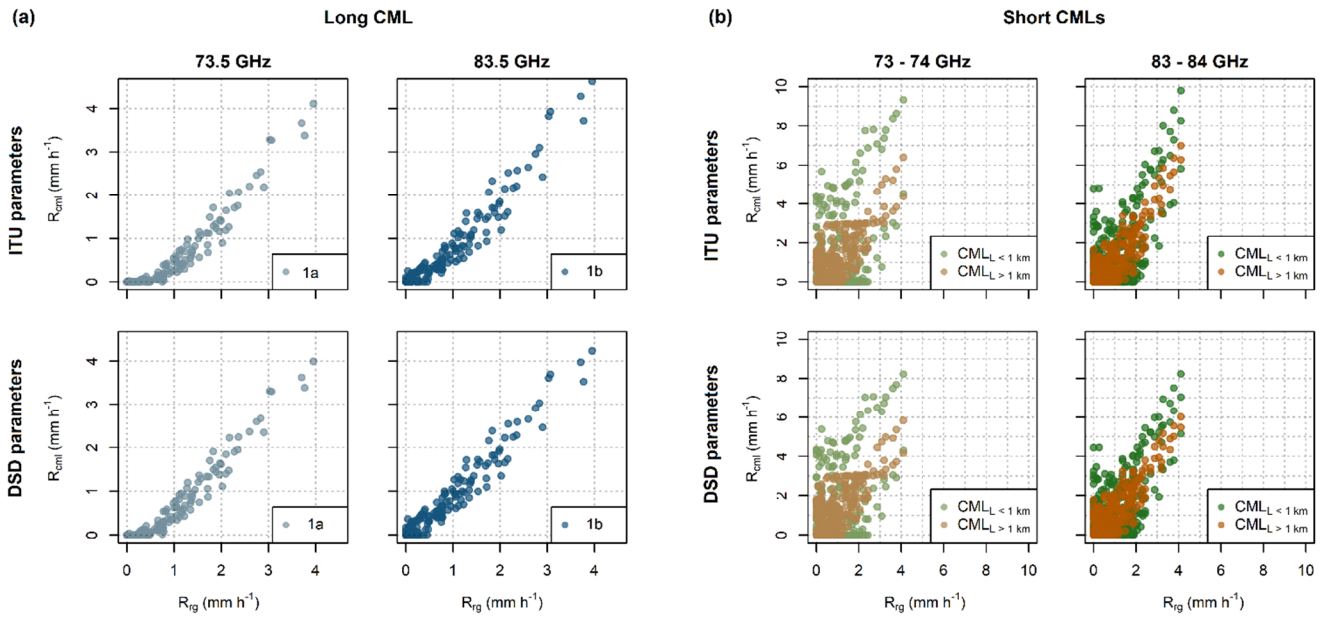

Figure 11: CML QPEs for the long CML (a) and short (b) CMLs when using k-R model with ITU (top) and DSD-derived (bottom) parameters. Results are shown for both frequency ranges. QPEs for short CMLs are differentiated by color into two groups to depict CMLs with path lengths shorter and longer than 1 km separately.

Table 5: Performance metrics of the CML QPEs obtained with the k-R model using ITU and DSD-derived parameters

Sub-link	ITU parameters	DSD parameters

id	r (-)	rel. error (-)	RMSE (mm h^{-1})	r (-)	rel. error (-)	RMSE (mm h^{-1})
1a	0.95	-0.44	0.49	0.96	-0.35	0.39
1b	0.96	-0.17	0.31	0.97	-0.08	0.24
2a	0.86	0.10	0.64	0.86	0.23	0.64
2b	0.87	0.26	0.75	0.87	0.33	0.69
3a	0.67	0.34	0.92	0.66	0.43	0.97
3b	0.84	0.15	0.71	0.83	0.21	0.69
4a	0.74	-0.48	0.95	0.74	-0.44	0.92
4b	0.78	0.24	1.31	0.77	0.26	1.14
5a	0.73	-0.78	0.92	0.74	-0.77	0.90
5b	0.80	-0.61	0.79	0.81	-0.59	0.76
6a	0.57	1.26	2.29	0.53	1.25	2.18
6b	0.63	0.61	1.56	0.61	0.59	1.44

In general, rainfall retrieval by E-band CMLs is affected during light rainfalls not only by deficiencies related to WAA and the baseline, but also deficiencies related to DSD. WAA and baseline-related errors clearly dominate by shorter CMLs, whereas regarding the 4.86-km-long CML, DSD seems to have a similar or~~,~~ even larger effect (in the case of the 83.5 GHz sub-link~~, even larger effect.~~). The effect of DSD is likely to increase with high rainfall intensities, which were, however, not encountered during the case study period.

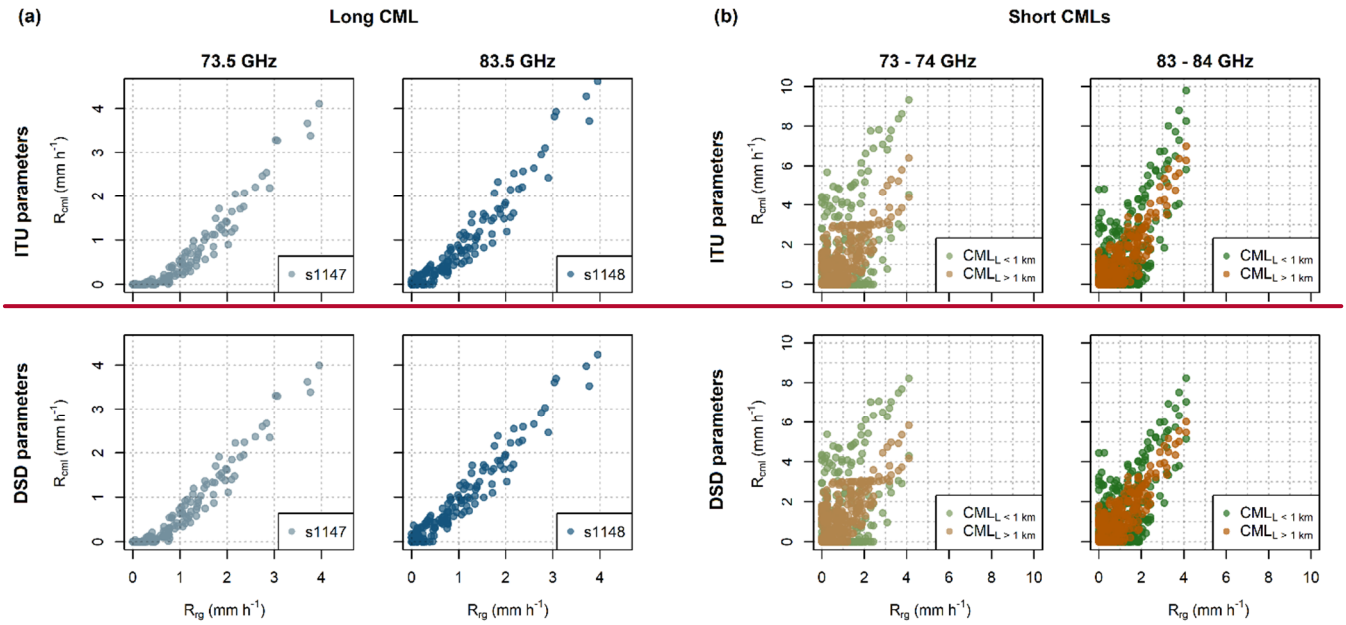

5 ~~Figure 11: CML QPEs for the long CML (a) and short (b) CMLs when using k-R model with ITU (top) and DSD-derived (bottom) parameters. Results are shown for both frequency ranges. QPEs for short CMLs are differentiated by color into two groups to depict CMLs with path lengths shorter and longer than 1 km separately.~~

~~Table 5: Performance of the CML QPEs obtained with the k-R model using ITU and DSD-derived parameters~~

~~Sub-link~~	~~ITU parameters~~			~~DSD parameters~~		
~~id~~	~~r (-)~~	~~rel. error (-)~~	~~RMSE (mm h^{-1})~~	~~r (-)~~	~~rel. error (-)~~	~~RMSE (mm h^{-1})~~
~~1147~~	~~0.95~~	~~-0.44~~	~~0.49~~	~~0.96~~	~~-0.35~~	~~0.39~~
~~1148~~	~~0.96~~	~~-0.17~~	~~0.31~~	~~0.97~~	~~-0.08~~	~~0.24~~
~~3007~~	~~0.73~~	~~-0.78~~	~~0.92~~	~~0.74~~	~~-0.77~~	~~0.90~~
~~3006~~	~~0.80~~	~~-0.61~~	~~0.79~~	~~0.81~~	~~-0.59~~	~~0.76~~
~~3008~~	~~0.57~~	~~1.26~~	~~2.29~~	~~0.53~~	~~1.25~~	~~2.18~~
~~3009~~	~~0.63~~	~~0.61~~	~~1.56~~	~~0.61~~	~~0.59~~	~~1.44~~
~~3050~~	~~0.67~~	~~0.34~~	~~0.92~~	~~0.66~~	~~0.43~~	~~0.97~~
~~3051~~	~~0.84~~	~~0.15~~	~~0.71~~	~~0.83~~	~~0.21~~	~~0.69~~
~~3004~~	~~0.86~~	~~0.10~~	~~0.64~~	~~0.86~~	~~0.23~~	~~0.64~~
~~3005~~	~~0.87~~	~~0.26~~	~~0.75~~	~~0.87~~	~~0.33~~	~~0.69~~
~~3010~~	~~0.74~~	~~-0.48~~	~~0.95~~	~~0.74~~	~~-0.44~~	~~0.92~~
~~3011~~	~~0.78~~	~~0.24~~	~~1.31~~	~~0.77~~	~~0.26~~	~~1.14~~

5 Discussion

Gaseous attenuation: The theoretical gaseous attenuation for 73.5 GHz sub-link ranges between 1.33 dB and 2.90 dB (amplitude 0.33 dB km^{-1}) and for the 83.5 GHz sub-link between 0.95 dB and 3.06 dB (amplitude 0.45 dB km^{-1}). These fluctuations have a minor effect on rainfall retrieval (with respect to uncaptured baseline variability), as 0.33, resp. 0.45- dB km^{-1} corresponds to a rainfall intensity of about 0.19 mm h^{-1} resp. 0.25 mm h^{-1} for 73.5 GHz and 83.5 GHz sub-links. On the other hand, this signal is sufficiently strong to enable the detection of water vapor at long CMLs, as 0.33 dB km^{-1} ~~resp.~~and 0.45 dB km^{-1} corresponds ~~to~~by the long CML (4.86 km) of 1.60 dB resp. 2.19 dB. The major challenge lies in the separation of gaseous attenuation from losses caused by other phenomena. This is easier during periods without rainfall, nevertheless, the following causes of losses need to be identified and separated.

First, WAA occurring after rainfall and during dew events can reach 4 dB, *i.e.*, substantially exceeds the gaseous ~~attention~~attenuation. Here, a safety window of 6 h size was used before and after each rain gauge tipping to exclude periods with WAA contribution. This mostly eliminated WAA before and after rainfall events and WAA during strong dew events causing a rain-gauge ~~tippings~~tip. However, such eliminations considerably reduce ratio of time intervals with observations. Moreover, periods before and after rainfalls might have higher relative humidity than average and discarding those from the evaluation leads to potentially biased long-term estimates of water vapor density.

Second, signal fluctuations due to multipath propagation or other sources of uncertainty might affect the observed attenuation level. ~~So-called multipath interference occurs~~Multipath ~~due to the constructive or destructive phase summation of the signal at the receiving antenna during the atmospheric multipath propagation conditions (Valtr et al., 2011). Such interferences often lead to a decreased signal power level of one sub-link while keeping the signal power level of the other sub-link.~~ interferences often lead to a decreased signal power level of one sub-link while keeping the signal power level of the other sub-link (Valtr et al., 2011).

Finally, hardware related artifacts might destroy a gaseous attenuation signal. For example, sub-link ~~3008~~6a drifts about 1.5 dB during the period from the end of October to mid-December. This drift is clearly related to the hardware as the total loss due to gaseous attenuation along the path length of 0.39 km can reach only about 0.13 dB. Such a drift would, however, make the quantification of gaseous attenuation impossible even at long CMLs.

The separation of gaseous attenuation from other sources of signal loss is challenging. Further research could take advantage of the 10 GHz duplex separation between the sub-links of E-band CMLs. Combining attenuation information from CMLs of different lengths might also be promising.

Accuracy of the k-R power law approximation: The relation between rainfall and raindrop attenuation (~~4, 5~~Eq. 7 and 8) on E-band frequencies is substantially more dependent on DSD than on 15–40 GHz CMLs (Chwala, 2017). The parameters of the power-law model (~~5~~Eq. 8), when optimized for all the DSD data, corresponds extremely well to the ITU parameters ~~(ITU-R P.838-3, 2005). However, high~~(ITU-R, 2005). However, high values of RMSE results from the variability in DSD when using one fit for all the records. Separate fits for convective and stratiform rainfalls ~~reduce~~halve the RMSE ~~to half~~values.

Moreover, the separate power-law fits are closer to linear (~~beta~~parameter β between 1.18 and 1.26, compared to ~~beta~~β between 1.38 and 1.4) and are less prone to errors related to non-uniform rainfall distribution along the CML path. Errors due to non-linearity of ~~relation (5~~Eq. (8) might be reduced by reconstructing rainfall spatial variability along the CML path from the neighboring CMLs, or by introducing a climate-based relation between the non-uniformity of rainfall distribution and rainfall intensity. Such methods will, however, require further research. In general, unknown DSD will probably be one of the major uncertainties in quantitative estimates of heavy rainfall. On the other hand, high sensitivity to DSD creates the opportunity to infer information on DSD from the attenuation of E-band CMLs, *e.g.*, in a condensed form of DSD moments. This is, in theory, also possible at 15–40 GHz, though difficult to accomplish in practice (Leth et al., 2019). Additional information on rainfall intensity or a combination with attenuation data of CMLs operating at lower frequencies will be required for DSD retrieval.

Quality check before rainfall retrieval: Quality check was performed through visually inspecting time series of total losses. In the case of CML 2 a sudden change in baseline by 2 dB was manually corrected. More details to hardware related artifacts is provided in *Appendix B*.

Dry-wet weather classification and baseline separation:

The dry-wet classification has been reported as an important step in CML pre-processing as it minimizes unwanted changes in attenuation level by setting the baseline separately for each event from the relatively short period before the event (Chwala and Kunstmann, 2019; Overeem et al., 2011). Here, dry-wet weather classification was not used for baseline identification. It was a pragmatic choice enabling better descriptions of the WAA effect. Dry-wet classification is also needed for filtering out periods with increased attenuation due to WAA (after rainfall and during dew events), nevertheless, these periods are in the event-based evaluation not included.

The separation of wet weather (including dew occurrence) was identified as a crucial step when analyzing attenuation due to water vapor. When rain gauges are not available a CML-based classification needs to be performed. The dry-wet weather classification ~~used~~ (Schleiss and Berne, 2010) used in *Appendix A* is designed to identify rainy periods and consider dew occurrences as dry weather. Although sensitivity to dew events can be increased by optimizing the parameters of the algorithm, dew events have similar dynamics as changes in air humidity as they are both dependent on temperature. Thus, other methods also considering observations of neighboring CMLs (Overeem et al., 2011) might be more appropriate for the dry-wet weather classification used for the separation of attenuation caused by water vapor.

~~It should be noted that, with the exception of one case, the observed attenuation levels were stable and the~~The baseline identification method with a moving median (without dry-wet weather classification) performed well for rainfall retrieval purposes. ~~The~~It should be noted that, with the exception of one case, the observed attenuation levels were stable. The median moving window baseline with window size of one week was capable to correct long-term drift, which occurred on sub-link 6a (*Appendix B*). Window size of one week is sufficiently long to not include more than 50 % of wet weather records into the window at any time step in the temperate climate. However, the median moving window baseline is not suitable for distinguishing between long-term drift related to hardware malfunction (*e.g.*, sub-link ~~3008~~6a) and drift related to seasonal changes in air humidity and temperature (sub-links ~~1147~~1a and ~~1148).~~1b). Constant baseline was, therefore, used for analysis

of gaseous attenuation on sub-links 1a and 1b instead. Possible water vapor monitoring thus poses higher requirements on the hardware with respect to the stability of the attenuation baseline. ~~Note, our results are hardware-specific and based on four months of CML records only.~~

Wet antenna attenuation: Quantification of WAA during rainfall is based on the assumption that rainfall has a uniform distribution over the study area, and that water formation on the surface of antenna radomes is the same for both the short CMLs and the long one. In our case, the first assumption holds well as all four rain gauges observe similar rainfall intensities during the evaluated events. The correlation coefficient between rain gauges ~~rg_~~at sites 1, ~~rg_~~2 and ~~rg_~~4, which are closer to each other, is 0.94–0.96 and 0.88–0.93 for the more distant ~~rg_3.~~rain gauge at site 3. The similarity in antenna characteristics, *i.e.* hydrophobic properties of antenna radomes as well as their actual status, was not inspected directly. That said, the estimation procedure is relatively insensitive to WAA occurring on the long CML as attenuation along its path dominates over WAA, even during relatively light rainfalls and, thus, WAA does not significantly influence the estimated specific attenuation (~~12~~13).

WAA during rainfall is weakly correlated to rainfall intensity (*e.g.*, Schleiss et al., 2013). Our results are limited to light and moderate rainfall only. Schleiss et al. (2013) reported drying of up to six hours with an exponential decrease of WAA, which also corresponds well to our observations (Fig. ~~7~~9a). However, quantification of exact durations of drying require additional instrumentation to enable us to determine ends of rainfalls directly. The exponential WAA decrease during drying was also reported by Leth et al. (2018) who suggested that this drying pattern occurs on antennas with non-degraded coating, which is also the case of the CML antennas ~~anlayzed here.~~analyzed. On the other hand, WAA attenuation patterns on antennas with degraded coating might be markedly different.

WAA due to water vapor condensation reaches higher values than during light rainfall. This might be caused by an absence of water rivulets (Leth et al., 2018). The higher values of attenuation caused by water droplets, in comparison to attenuation caused by rivulets, was also reported by Mancini et al. (2019). Comparable attenuation patterns of light rainfall and water vapor condensation may cause the misclassification of dew as rainfall.

In general, WAA quantified in this study is slightly higher than WAA reported for lower frequencies (Leth et al., 2018). However, the relative contribution of WAA to the total attenuation is less significant (given the high sensitivity of CMLs to raindrop path attenuation). WAA is, thus, a smaller source of possible bias than on 15–40 GHz frequencies, nevertheless, its accurate quantification is still important, especially for shorter CMLs. In addition, WAA during heavy rainfalls was not investigated in this study and might be higher, as was shown for lower frequencies by ~~(Fencl et al., 2019)~~Fencl et al. (2019).

Rainfall estimation ~~**and effect of drop size distribution:**~~

: The E-band CMLs proved to be markedly more sensitive to raindrop path attenuation than 15–40 GHz devices. The long CML provided surprisingly accurate rainfall estimates, even for light rainfalls lower than 1 mm h^{-1} in intensity (Fig. 11). Assuming a detection threshold of 1 dB (typical *tx* power quantization of older devices), a 1-km-long 83~~_~~GHz CML can already detect rainfall intensity of 0.6~~—~~1 mm h^{-1} depending on rainfall type, whereas, *e.g.*, a 23 GHz or 38 GHz CML ~~(typical for older networks)~~ only detects rainfalls heavier than 8.4 resp. 3.6 mm h^{-1}, *i.e.,* the sensitivity to light rainfalls is almost an

order of magnitude higher for E-band CMLs. Moreover, the quantization of *rx* and *tx* records has improved to 0.1 dB with E-band CMLs. On the other hand, long E-band CMLs are prone to outages (*rx* drops under detection level) during heavy rainfall. This high sensitivity to rainfall, together with improved quantization, opens the opportunity for monitoring rainfall with CMLs having a sub-kilometer path length, which was practically not possible before without adjusting CML QPEs to the rain gauges (Fencl et al., 2017). Short CMLs are more affected by errors related to WAA, yet the influence of WAA is relatively smaller during heavier rainfall, which, ~~unfortunately~~however, did not occur during the evaluation period. The use of short CMLs may be convenient, especially during heavy rainfalls associated with high spatial variability by which an assumption about uniform rainfall distribution along a CML path is more likely valid than for long CMLs. Reliable rainfall estimation from short CMLs, however, requires further research on WAA modeling at E-band frequencies.

Limitations of this study: The study investigates the weather monitoring capabilities of E-band CMLs on a dataset comprised of four months of attenuation data from six Ericsson MINILINK CMLs operated within cellular backhaul. The number of CMLs and length of the period is sufficient to demonstrate the challenges and opportunities related to rainfall and water vapor monitoring at an E-band. ~~The~~However, the limited size of the dataset does not enable us to draw strong conclusions on the overall reliability of weather monitoring with an E-band, nor to investigate in detail new opportunities related to CML sensitivity to water vapor and DSD.

Specifically, the dataset does not include heavy rainfalls. The reliability of E-band CML rainfall estimation for heavy rainfalls is based only on the evaluation of theoretical attenuations obtained from DSD observations (Duebendorf). The DSD effect on the attenuation-rainfall relation could not be, therefore, studied in detail on the observed CML data. Finally, air temperature and humidity are measured at two locations close to one node of the CML path. Despite these limitations, we believe that the presented results reliably demonstrate new challenges and opportunities of E-band CML weather monitoring.

6 Conclusions

E-band microwave links are increasingly updating and frequently replacing the older hardware of backhaul networks operating mostly at 15–40 GHz. This investigation demonstrates new challenges and opportunities related to CML weather monitoring. The principles behind weather retrieval is the same as for lower frequency bands, nevertheless the influence of atmospheric phenomena such as drop size distribution, or changes in air temperature and humidity affect radiowave propagation in a significantly different manner. Furthermore, hardware used by E-bands is different (quantization, accuracy, antenna wetting, etc.). The results, obtained from simulations and the case study with attenuation data from real-world CMLs, are encouraging. The main conclusions are listed below:

- E-band CMLs are ~~by about one order of magnitude~~markedly more attenuated by raindrops along their path than older 15–40- GHz devices, during lighter rainfalls by about 20 times more than 15 GHz and 2 - 3 times more than 40 GHz devices. This significantly improves the ability of E-band CMLs to quantify rainfall intensity accurately during light rainfalls.

- The rainfall retrieval at E-band frequencies is less influenced by wet antenna attenuation than ~~by~~at lower frequencies. WAA observed in this study has a similar pattern as that described by ~~(Schleiss et al., 2013)~~Schleiss et al. (2013), *i.e.*, it is almost uncorrelated with rainfall intensity and exhibits an exponential decrease after rainfall lasting up to several hours. WAA during dew occurrences reaches up to 4 dB.
- The power-law approximation of the attenuation-rainfall relation depends substantially more on DSD than on 15–40 GHz frequencies. The variability in DSD represents significant uncertainties in E-band CML rainfall retrieval. Use of different parameter sets for different types of rainfall, as done with weather radars, reduce DSD-related errors, nevertheless this requires additional information on rainfall type.
- The k-R relation at E-band frequencies is less linear than at lower frequencies. This might cause errors, especially by longer CMLs, for which a uniform distribution of rainfall intensity along their path cannot always be assumed. On the other hand, even short (sub-kilometer) E-band CMLs are sufficiently sensitive to raindrop path attenuation to be used for rainfall retrieval.
- Gaseous attenuation at E-band CMLs is detectable, however, it is ~~two orders of magnitude~~ substantially smaller than attenuation due to rainfall. Fluctuations in specific attenuation caused by water vapor typically not exceed 1 dB km^{-1} in the region of temperate climate. This magnitude is reached by rainfall with intensity around 1 mm h^{-1}. Gaseous attenuation is driven mainly by water vapor density and is, thus, in theory, an accurate predictor of this atmospheric variable. This, however, requires the efficient separation of attenuation from other signal losses which is, in practice, challenging. Our first results show that this separation is, to some extent, possible during dry weather periods, if a sufficiently long CML (several km) is available.

In general, the ongoing shift of CML networks towards higher frequencies creates opportunities for the monitoring of rainfall on a qualitatively different level. New E-band CMLs are able to observe ~~even~~ light rainfalls and, in combination with lower frequency CMLs, potentially serve as DSD predictors. The rainfall retrieval methods developed for CMLs operating at 15–40 GHz frequencies proved to be useful for E-band CMLs as well. Water vapor retrieval from E-band CMLs having a path length of several kilometers might be possible, although the efficient separation of gaseous attenuation from other signal losses will be challenging in practice. This first experience with E-band CML weather retrieval, as presented in this study, will hopefully contribute to more robust designs of future experimental studies and case studies investigating this new technology with respect to weather monitoring.

~~**4.1 Dry-wet classification**~~

Appendix A – Dry-wet weather classification~~:~~

The classification is performed separately for each sub-link on quality-checked total observed losses ~~using the~~. The algorithm of ~~(Schleiss and Berne, 2010)~~Schleiss and Berne (2010) is used which is based on a moving window standard deviation. The window size is set to 15 minutes and the threshold for classifying the record as wet (σ_0) is set to the 94 % quantile of all

standard deviations resulting from the moving window filter. The 94 % probability corresponds approximately to the wet weather ratio in the Prague data as classified by the rain gauges.

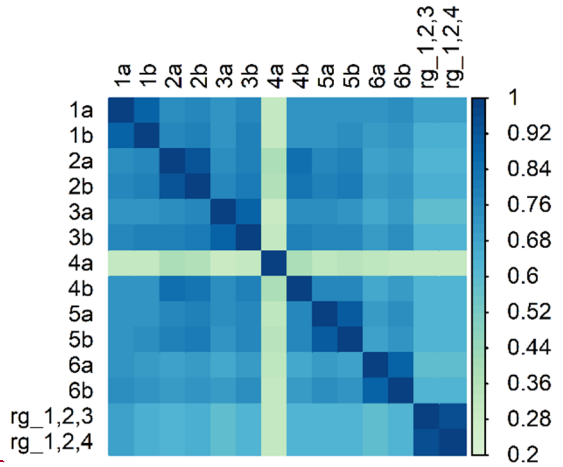

~~Dry-wet weather classification:~~

~~Figure A1: Statistical relationship between dry-wet classifiers based on single CML sub-links and rain gauges along the path of the long CML (rg_1,2,3) and three rain gauges near five shorter CMLs (rg_1,2,4) expressed by correlation coefficient.~~

Dry-wet weather classifiers obtained from CML sub-links are compared with each other and with classifiers obtained from rain gauge observations. Correlation is used here as a measure of similarity. The evaluation of dry-wet weather is performed on one-minute data because precise identification of the onset and ending of rainfall significantly affects baseline identification methods based on dry wet classification, as well as the quantification of wet antenna attenuation.

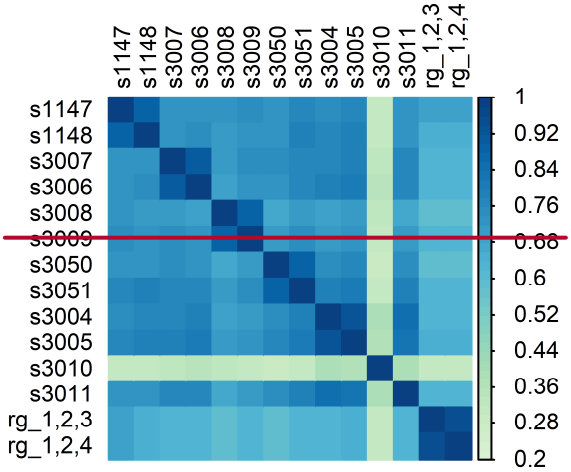

~~Figure 6: Statistical relationship between dry-wet classifiers based on single CML sub-links and rain gauges along the path of the long CML (wet_rg1,2,3) and three rain gauges near five shorter CMLs (wet_rg1,2,4) expressed by correlation coefficient.~~

Dry-wet weather classifiers of single sub-links belonging to one CML are strongly correlated (Fig. ~~6~~A1). An exception is sub-link ~~30104~~a which is affected by a hardware malfunction (~~degraded resolution~~*Appendix B*). The correlation between the classifiers of sub-links belonging to different CMLs is lower but still reaches high values ranging between r = 0.57 and r =

0.84. The correlation of CML classifiers to the classifiers based on rain gauges is, on average, slightly lower (r = 0.57–0.67). ~~In general, the CMLs tend to detect rainfall earlier than rain gauges. It can be attributed to the delay of rain gauge rain detection due to the filling of the bucket.~~

The evaluation of dry-wet weather classification is only approximate because tipping bucket rain gauges are unable to detect the exact beginning or end of a rain event. Visual inspection of time series reveals that disagreement between rain gauges and CMLs occur most commonly during dew events and during periods of low temperature where mixed or snow events probably occur. Although sensitivity to dew events can be increased by optimizing the parameters of the algorithm, dew events have similar dynamics as changes in air humidity as they are both dependent on temperature. Thus, other methods also considering observations of neighboring CMLs (Overeem et al., 2011) might be more appropriate for the dry-wet weather classification used for the separation of attenuation caused by water vapor.

~~Identifying hardware~~ Appendix B – Hardware-related artifacts

There have been three types of hardware-related artifacts identified (visually) in the Prague data (Fig. ~~5~~B1): a) a sudden change in L_t, b) long-term gradual L_t drift, and c) 'degraded resolution'. 'Degraded resolution' is defined as behavior where *tx* and *rx* change with considerably lower frequency than is common with other CMLs. The degraded resolution can be easily recognized visually as a time series with no signal fluctuation within intervals of several hours.

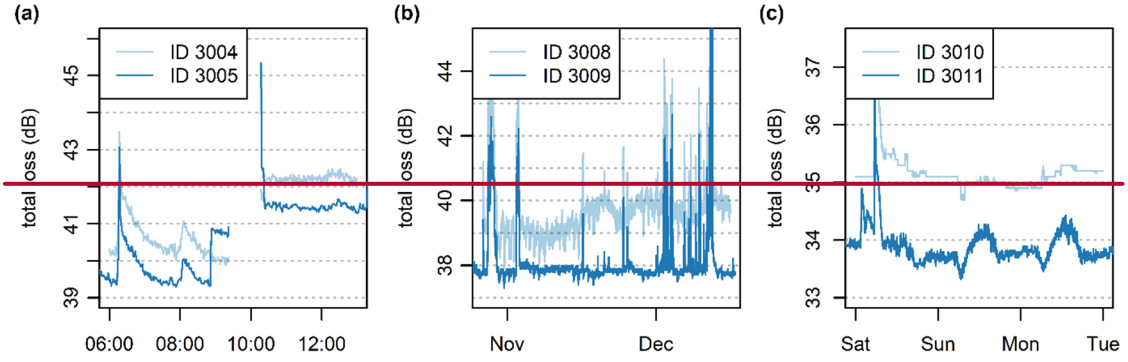

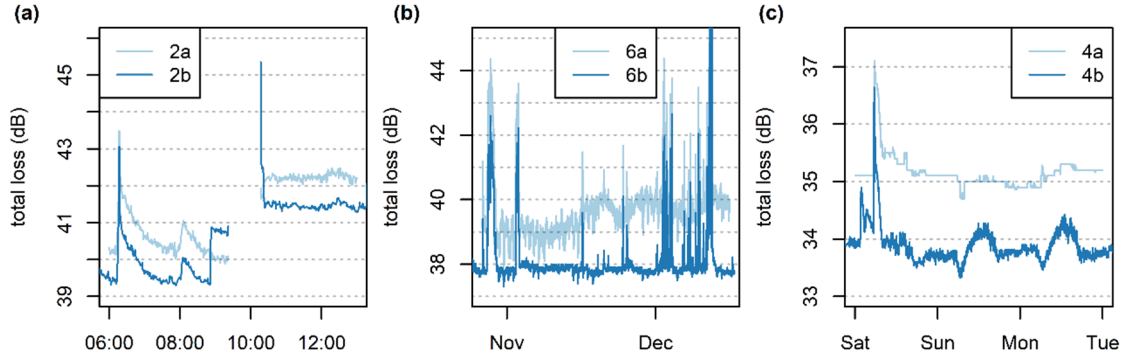

Figure ~~5~~B1: Demonstration of hardware related ~~artefacts~~artifacts (a) sudden change in the baseline of CML ~~3004_3005~~2, (b) baseline drift of sub-link ~~3008,~~6a and (c) degraded resolution of sub-link ~~3010~~4a.

The sudden change in L_t of about 2 dB occurred on CML ~~3004_3005~~2 on both sub-links (Fig. ~~5a~~ B1a). The change in baseline level was proceeded by approx. two hours of an outage ~~and is probably related to the slight displacement of the CML unit during maintenance work.~~. The long-term gradual drift of L_t occurred on sub-link ~~3008.~~6a (Fig. B1b). L_t levels observed during dry weather increased gradually, on average, ~~to~~by about 1.5 dB during the experimental period. Finally, sub-link ~~3010~~4a was affected during the whole experimental period by a degraded resolution~~.~~ (Fig. B1c). Interestingly, the degraded resolution was more pronounced during dry weather periods than rainy ones.

In general, attenuation levels during dry weather are relatively stable with respect to long-term drift (in the order of weeks). It holds for all CMLs except the 73 GHz sub-link of CML ~~3008_3009~~6 which has dry weather attenuation levels of about 1.5 dB higher at the end of the period compared to the beginning (Fig. ~~5b~~B1b). The most significant fluctuations in the baseline occur during dew events when water film forming on the CML antennas causes wet antenna attenuation (~~see subsection~~section 4.~~4~~3). The baseline fluctuations related to water vapor are presented in ~~subsection~~section 4.~~6.~~1 (Fig. 5).

~~**Hardware related artifacts:**~~ The hardware related artifacts identified in the E-band attenuation time series are similar to those occurring on ~~older~~ 15–40 GHz CMLs. The 'degraded resolution' can be identified easily by analyzing attenuation variability within (sub)hourly subsets. Detecting (and correcting for) the sudden change in attenuation level will be especially challenging in operation mode when attenuation needs to be processed in real-time. Long-term drift can be captured very well and corrected using a median moving window with a size of one week. Such a size of window is sufficiently long to not include more than 50 % of wet weather records into the window at any time step in the temperate climate~~.~~

Supplement link (will be included by Copernicus).

Code and data availability. The code for Prague data analysis and Prague data are publically available at Zenodo repository DOI 10.5281/zenodo.3632095. Duebendorf data (disdrometer observations) and the code are available upon request from the corresponding author.

Author contribution. MF and VB. designed the study layout. Data was collected by MF, VB and MD. Analysis was performed by MF with contribution of MD, MG, and PV. MF prepared the manuscript with contribution of all co-authors.

Competing interests. The authors declare that they have no conflict of interest.

Acknowledgements. This work was supported by the ~~project~~projects of Czech Science Foundation (GACR) No. 17-16389S and No. 20-14151J. We would like to thank T-Mobile Czech Republic a.s. for kindly providing us CML data and specifically to Pavel Kubík, for assisting with our numerous requests. Special thanks are extended to Prazska vodohospodarska spolecnost a.s. for providing rainfall data from their rain gauge network and Prazske vodovody a kanalizace, a.s. who carefully maintained the rain gauges. Last, but not least, we would like to thank Eawag for supporting COMMON project and Dr. Christian Chwala from Karlsruhe Institute of Technology (KIT) and University of Augsburg for supporting our analysis by calculating extinction cross-sections and providing Python implementation of Liebe model for calculating attenuation due to water vapor.

References

Atlas, D. and Ulbrich, C. W.: Path- and Area-Integrated Rainfall Measurement by Microwave Attenuation in the 1–3 cm Band, J. Appl. Meteor., 16(12), 1322–1331, doi:10.1175/1520-0450(1977)016<1322:PAAIRM>2.0.CO;2, 1977.

Berne, A. and Uijlenhoet, R.: Path-averaged rainfall estimation using microwave links: Uncertainty due to spatial rainfall variability, Geophys. Res. Lett., 34(7), L07403, doi:10.1029/2007GL029409, 2007.

Chwala, C.: Precipitation and humidity observation using a microwave transmission experiment and commercial microwave links, [online] Available from: https://opus.bibliothek.uni-augsburg.de/opus4/frontdoor/index/index/docId/37908 (Accessed 2 December 2019), 2017.

Chwala, C. and Kunstmann, H.: Commercial microwave link networks for rainfall observation: Assessment of the current status and future challenges, Wiley Interdisciplinary Reviews: Water, 6(2), e1337, doi:10.1002/wat2.1337, 2019.

Chwala, C., Keis, F. and Kunstmann, H.: Real-time data acquisition of commercial microwave link networks for hydrometeorological applications, Atmos. Meas. Tech., 9(3), 991–999, doi:10.5194/amt-9-991-2016, 2016.

David, N., Alpert, P. and Messer, H.: Technical Note: Novel method for water vapour monitoring using wireless communication networks measurements, Atmospheric Chemistry and Physics, 9(7), 2413–2418, doi:https://doi.org/10.5194/acp-9-2413-2009, 2009.

Ericsson: Ericsson Microwave Outlook, [online] Available from: https://www.ericsson.com/assets/local/microwave-outlook/documents/ericsson-microwave-outlook-report-2016.pdf (Accessed 15 July 2017), 2016.

Ericsson: Ericsson Microwave Outlook Report - 2018, [online] Available from: https://www.ericsson.com/en/reports-and-papers/microwave-outlook/reports/2018 (Accessed 10 December 2019), 2018.

Ericsson: Ericsson Microwave Outlook Report - 2019, [online] Available from: https://www.ericsson.com/en/reports-and-papers/microwave-outlook/reports/2019 (Accessed 10 December 2019), 2019.

Fencl, M., Dohnal, M., Rieckermann, J. and Bareš, V.: Gauge-adjusted rainfall estimates from commercial microwave links, Hydrol. Earth Syst. Sci., 21(1), 617–634, doi:10.5194/hess-21-617-2017, 2017.

Fencl, M., Valtr, P., Kvičera, M. and Bareš, V.: Quantifying Wet Antenna Attenuation in 38-GHz Commercial Microwave Links of Cellular Backhaul, IEEE Geoscience and Remote Sensing Letters, 16(4), 514–518, doi:10.1109/LGRS.2018.2876696, 2019.

Fencl, M., Dohnal, M. and Bareš, V.: Raw and preprocessed data for the paper Atmospheric Observations with E-band Microwave Links – Challenges and Opportunities, , doi:10.5281/zenodo.3632095, 2020.

Fujiwara, M.: Raindrop-size Distribution from Individual Storms, J. Atmos. Sci., 22(5), 585–591, doi:10.1175/1520-0469(1965)022<0585:RSDFIS>2.0.CO;2, 1965.

Hansryd, J., Li, Y., Chen, J. and Ligander, P.: Long term path attenuation measurement of the 71–76 GHz band in a 70/80 GHz microwave link, in Proceedings of the Fourth European Conference on Antennas and Propagation, pp. 1–4., 2010.

Hong, E. S., Lane, S., Murrell, D., Tarasenko, N. and Christodoulou, C.: Mitigation of Reflector Dish Wet Antenna Effect at 72 and 84 GHz, IEEE Antennas and Wireless Propagation Letters, 16, 3100–3103, doi:10.1109/LAWP.2017.2762519, 2017.

Humphrey, M. D., Istok, J. D., Lee, J. Y., Hevesi, J. A. and Flint, A. L.: A New Method for Automated Dynamic Calibration of Tipping-Bucket Rain Gauges, J. Atmos. Oceanic Technol., 14(6), 1513–1519, doi:10.1175/1520-0426(1997)014<1513:ANMFAD>2.0.CO;2, 1997.

Internationale Fernmelde-Union, Ed.: Handbook radiowave propagation information for desining terrestrial point-to-point links, Ed. 2008., ITU, Geneva., 2009.

~~ITU-R P.676-11: ITU-R P.676-11, [online] Available from: https://www.itu.int/dms_pubrec/itu-r/rec/p/R-REC-P.676-11-201609-I!!PDF-E.pdf, 2016.~~

~~ITU-R P.838-3~~ITU-R: ITU-R P.838-3, [online] Available from: http://www.itu.int/dms_pubrec/itu-r/rec/p/R-REC-P.838-3-200503-I!!PDF-E.pdf, 2005.

ITU-R: RECOMMENDATION ITU-R P.676-12 - Attenuation by atmospheric gases and related effects, [online] Available from: https://www.itu.int/dms_pubrec/itu-r/rec/p/R-REC-P.676-12-201908-I!!PDF-E.pdf, 2019.

Jaffrain, J. and Berne, A.: Experimental Quantification of the Sampling Uncertainty Associated with Measurements from PARSIVEL Disdrometers, J. Hydrometeor., 12(3), 352–370, doi:10.1175/2010JHM1244.1, 2010.

Jaffrain, J. and Berne, A.: Quantification of the Small-Scale Spatial Structure of the Raindrop Size Distribution from a Network of Disdrometers, J. Appl. Meteor. Climatol., 51(5), 941–953, doi:10.1175/JAMC-D-11-0136.1, 2012.

Leijnse, H., Uijlenhoet, R. and Stricker, J. N. M.: Rainfall measurement using radio links from cellular communication networks, Water Resour. Res., 43(3), W03201, doi:10.1029/2006WR005631, 2007.

Leijnse, H., Uijlenhoet, R. and Stricker, J. N. M.: Microwave link rainfall estimation: Effects of link length and frequency, temporal sampling, power resolution, and wet antenna attenuation, Advances in Water Resources, 31(11), 1481–1493, doi:10.1016/j.advwatres.2008.03.004, 2008.

Leth, T. C. van, Overeem, A., Leijnse, H. and Uijlenhoet, R.: A measurement campaign to assess sources of error in microwave link rainfall estimation, Atmospheric Measurement Techniques, 11(8), 4645–4669, doi:https://doi.org/10.5194/amt-11-4645-2018, 2018.

Leth, T. C. van, Leijnse, H., Overeem, A. and Uijlenhoet, R.: Estimating raindrop size distributions using microwave link measurements, Atmospheric Measurement Techniques Discussions, 1–27, doi:https://doi.org/10.5194/amt-2019-51, 2019.

Liebe, H. J., Hufford, G. A. and Cotton, M. G.: Propagation modeling of moist air and suspended water/ice particles at frequencies below 1000 GHz. [online] Available from: http://adsabs.harvard.edu/abs/1993apet.agar.....L (Accessed 17 October 2019), 1993.

Luini, L., Roveda, G., Zaffaroni, M., Costa, M. and Riva, C.: EM wave propagation experiment at E band and D band for 5G wireless systems: Preliminary results, in 12th European Conference on Antennas and Propagation (EuCAP 2018), pp. 1–5., 2018.

Mancini, A., Lebrón, R. M. and Salazar, J. L.: The Impact of a Wet S-Band Radome on Dual-Polarized Phased-Array Radar System Performance, IEEE Transactions on Antennas and Propagation, 67(1), 207–220, doi:10.1109/TAP.2018.2876733, 2019.

Messer, H., Zinevich, A. and Alpert, P.: Environmental Monitoring by Wireless Communication Networks, Science, 312(5774), 713–713, doi:10.1126/science.1120034, 2006.

Minda, H. and Nakamura, K.: High Temporal Resolution Path-Average Rain Gauge with 50-GHz Band Microwave, Journal of Atmospheric and Oceanic Technology, 22(2), 165–179, doi:10.1175/JTECH-1683.1, 2005.

Mishchenko, M. I. and Travis, L. D.: Capabilities and limitations of a current FORTRAN implementation of the T-matrix method for randomly oriented, rotationally symmetric scatterers, Journal of Quantitative Spectroscopy and Radiative Transfer, 60(3), 309–324, 1998.

Ostrometzky, J., Raich, R., Bao, L., Hansryd, J. and Messer, H.: The Wet-Antenna Effect—A Factor to be Considered in Future Communication Networks, IEEE Transactions on Antennas and Propagation, 66(1), 315–322, doi:10.1109/TAP.2017.2767620, 2018.

Overeem, A., Leijnse, H. and Uijlenhoet, R.: Measuring urban rainfall using microwave links from commercial cellular communication networks, Water Resources Research, 47(12), doi:10.1029/2010WR010350, 2011.

Schleiss, M. and Berne, A.: Identification of Dry and Rainy Periods Using Telecommunication Microwave Links, IEEE Geoscience and Remote Sensing Letters, 7(3), 611–615, doi:10.1109/LGRS.2010.2043052, 2010.

Schleiss, M., Rieckermann, J. and Berne, A.: Quantification and Modeling of Wet-Antenna Attenuation for Commercial Microwave Links, IEEE Geoscience and Remote Sensing Letters, 10(5), 1195–1199, doi:10.1109/LGRS.2012.2236074, 2013.

Ulbrich, C. W.: Natural Variations in the Analytical Form of the Raindrop Size Distribution, J. Climate Appl. Meteor., 22(10), 1764–1775, doi:10.1175/1520-0450(1983)022<1764:NVITAF>2.0.CO;2, 1983.

Valtr, P., Pechac, P., Kvicera, V. and Grabner, M.: Estimation of the Refractivity Structure of the Lower Troposphere From Measurements on a Terrestrial Multiple-Receiver Radio Link, IEEE Transactions on Antennas and Propagation, 59(5), 1707–1715, doi:10.1109/TAP.2011.2122234, 2011.

Wang, Z., Schleiss, M., Jaffrain, J., Berne, A. and Rieckermann, J.: Using Markov switching models to infer dry and rainy periods from telecommunication microwave link signals, Atmospheric Measurement Techniques, 5(7), 1847–1859, doi:10.5194/amt-5-1847-2012, 2012.

Woodhouse, I. H.: Introduction to microwave remote sensing, CRC press., 2017.